Additive manufacturing of vascular stents

Li, Yageng; Shi, Yixuan; Lu, Yuchen; Li, Xuan; Zhou, Jie; Zadpoor, Amir A.; Wang, Luning

DOI
10.1016/j.actbio.2023.06.014

Publication date
2023

Document Version
Final published version

Published in
Acta Biomaterialia

Acta Biomaterialia 167 (2023) 16–37

Contents lists available at ScienceDirect

Acta Biomaterialia

journal homepage: www.elsevier.com/locate/actbio

Review article

Additive manufacturing of vascular stents

Yageng Li[a], Yixuan Shi[a], Yuchen Lu[a], Xuan Li[a], Jie Zhou[b,*], Amir A. Zadpoor[b,*], Luning Wang[a,*]

[a] Beijing Advanced Innovation Center for Materials Genome Engineering, School of Materials Science and Engineering, University of Science and Technology Beijing, Beijing, 100083, China
[b] Department of Biomechanical Engineering, Delft University of Technology, Delft 2628 CD, the Netherlands

ARTICLE INFO

Article history:
Received 29 March 2023
Revised 11 June 2023
Accepted 13 June 2023
Available online 17 June 2023

Keywords:
Additive manufacturing
Biomaterial
Vascular stent
Mechanical property
Biological performance

ABSTRACT

With the advancement of additive manufacturing (AM), customized vascular stents can now be fabricated to fit the curvatures and sizes of a narrowed or blocked blood vessel, thereby reducing the possibility of thrombosis and restenosis. More importantly, AM enables the design and fabrication of complex and functional stent unit cells that would otherwise be impossible to realize with conventional manufacturing techniques. Additionally, AM makes fast design iterations possible while also shortening the development time of vascular stents. This has led to the emergence of a new treatment paradigm in which custom and on-demand-fabricated stents will be used for just-in-time treatments. This review is focused on the recent advances in AM vascular stents aimed at meeting the mechanical and biological requirements. First, the biomaterials suitable for AM vascular stents are listed and briefly described. Second, we review the AM technologies that have been so far used to fabricate vascular stents as well as the performances they have achieved. Subsequently, the design criteria for the clinical application of AM vascular stents are discussed considering the currently encountered limitations in materials and AM techniques. Finally, the remaining challenges are highlighted and some future research directions are proposed to realize clinically-viable AM vascular stents.

Statement of significance

Vascular stents have been widely used for the treatment of vascular disease. The recent progress in additive manufacturing (AM) has provided unprecedented opportunities for revolutionizing traditional vascular stents. In this manuscript, we review the applications of AM to the design and fabrication of vascular stents. This is an interdisciplinary subject area that has not been previously covered in the published review articles. Our objective is to not only present the state-of-the-art of AM biomaterials and technologies but to also critically assess the limitations and challenges that need to be overcome to speed up the clinical adoption of AM vascular stents with both anatomical superiority and mechanical and biological functionalities that exceed those of the currently available mass-produced devices.

1. Introduction

Vascular diseases are one of the biggest threats to human health [1]. With the gradual increases in life expectancy and population aging, this threat is projected to grow over time. Vascular diseases include cardiovascular diseases, cerebrovascular diseases, vascular trauma, and vascular defects. Among these, cardiovascular diseases are a group of disorders of heart and blood vessels, which comprise coronary heart disease (CHD), coronary artery disease (CAD), acute coronary syndrome (ACS), and peripheral arterial disease (PAD) [1]. Cerebrovascular diseases refer to a group of conditions that affect the blood flow and blood vessels in the brain, which may lead to ischemic or hemorrhagic stroke [2–4]. On the basis of a systematic analysis of population health data, cardiovascular and cerebrovascular diseases are identified as the leading causes of death globally [5]. In 2019, about 17.9 million people died from vascular diseases, accounting for 32% of all global deaths [6]. Among those deaths, 85% were due to heart attack and stroke, according to the World Health Organization (WHO) [7]. Heart attacks and strokes are mainly associated with a common pathophysiology involving atherosclerosis and thrombosis [8]. The most common cause is the build-up of fatty deposits and blood clots inside

* Corresponding authors.
E-mail addresses: j.zhou@tudelft.nl (J. Zhou), a.a.zadpoor@tudelft.nl (A.A. Zadpoor), luning.wang@ustb.edu.cn (L. Wang).

https://doi.org/10.1016/j.actbio.2023.06.014
1742-7061/

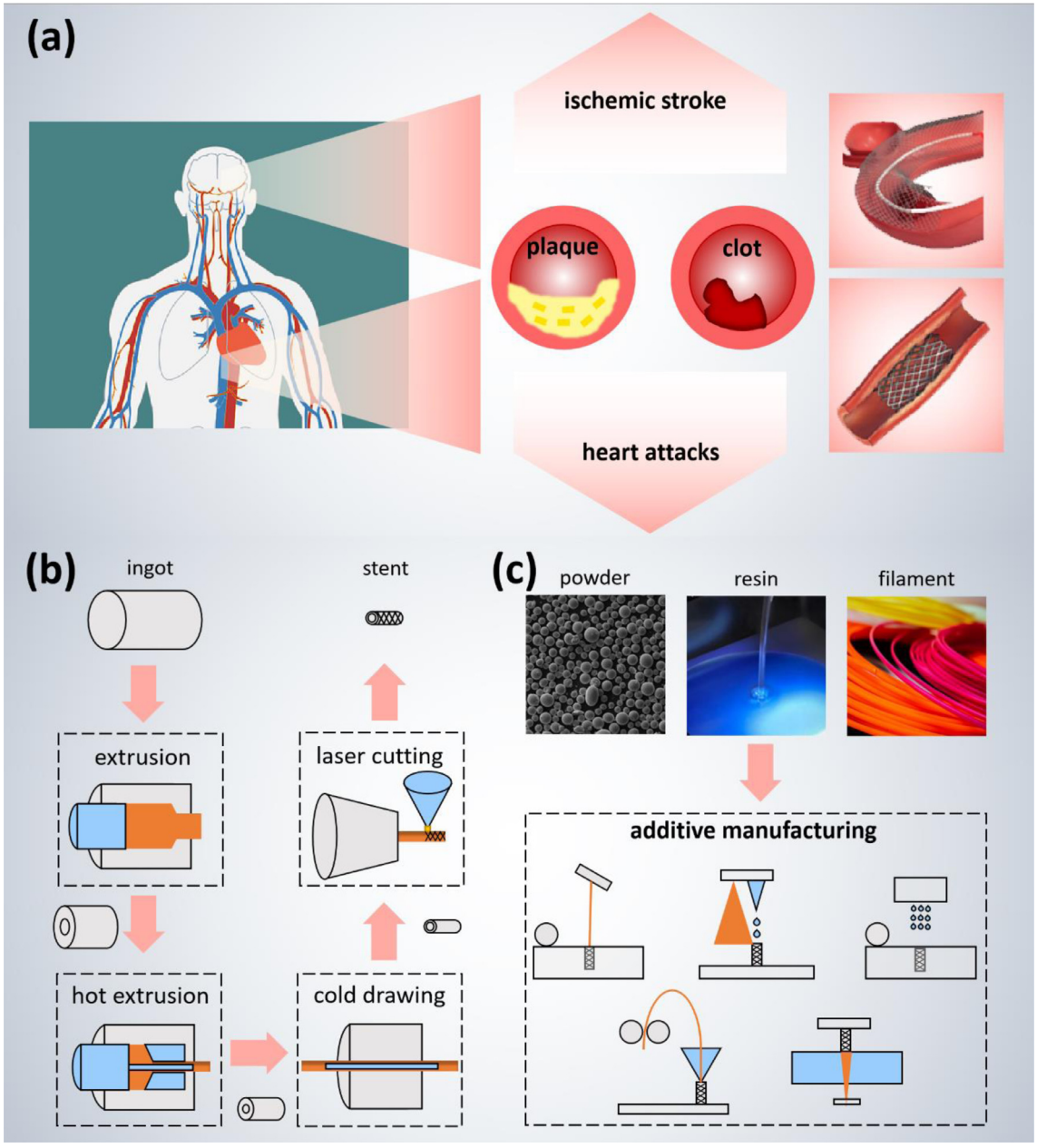

Fig. 1. Schematic diagrams of vascular diseases and stent fabrication: (a) cardiovascular and cerebrovascular diseases [4], (b) conventional fabrication of stent, and (c) AM of stent.

the blood vessels that restrict blood flow or fully block the flow of blood from the heart to the brain (Fig. 1**a**).

In addition to traditional drug therapies, the interventional approaches that are extensively used to treat vascular diseases have gradually advanced in the last four decades [9]. Endovascular stent is commonly used for the treatment of coronary heart diseases and stroke, due to their good performance in terms of vascular reconstruction [10,11]. Stent implantation is carried out through a procedure in which a cage-like mesh device is inserted into the affected area of the blood vessel. Once the target lesion is reached, the stent is deployed to open the narrowed or blocked vessel and provide sustained support, thereby restoring and maintaining the blood flow. Vascular stents may be fabricated from metals, polymers, or composites, typically with standardized shapes, sizes, and unit cell designs. However, the geometry of human blood vessels may vary from one person to another, which means a standard stent often do not perfectly match the patient's localized vascular defect [12]. On the other hand, with the conventional stent fabrication technologies, patient-specific and location-specific solutions are infeasible due to technological limitations and prohibitively high costs associated with the lengthy procedures required for the development and fabrication of conventional vascular stents, typically involving mini-tube manufacturing and laser cutting (Fig. 1**b**) [13] followed by surface treatments.

Additive manufacturing (AM) technologies present unprecedented opportunities for the healthcare sector because they enable the realization of patient-specific (implantable) devices, therapeutics, and instruments [14]. Since clinical outcomes can be significantly improved when patient's specific needs are met [14], there has been enormous interest in personalized medical treatments in the recent years. For instance, patient-specific orthopedic implants with high accuracy and geometrical complexity have been man-

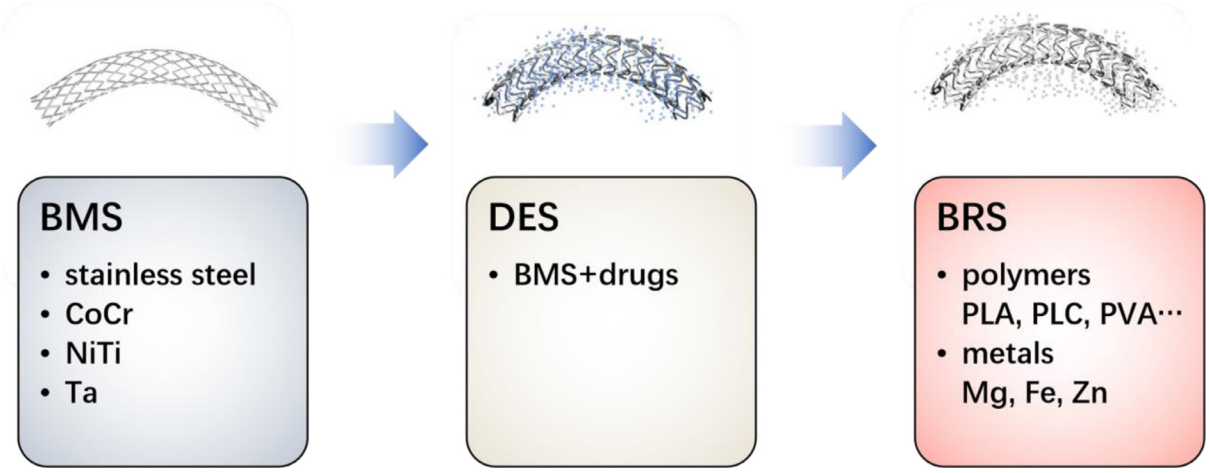

Fig. 2. Three stages of material development for vascular stents.

ufactured, taking advantage of the form-freedom offered by AM techniques [15]. With the increasing maturity of AM technologies in terms of achievable resolutions and processable biomaterials, the concept of AM vascular stents has received increasing attention during the last few years [16]. AM not only makes the fabrication of personalized vascular stents feasible and potentially cost-effective but can also alleviate the treatment failures caused by the poor conformability of the conventional stents. These advantages have motivated the exploration of the capabilities of AM biomaterials for the realization of patient-specific vascular stents (Fig. 1**c**). In this paper, we review the applications of AM biomaterials to the design and fabrication of vascular stents, paying particular attention to the recent advances in AM that could revolutionize vascular stents. This is an interdisciplinary subject area that has not been previously covered in published review articles [16,17]. Our objective is to not only present the state-of-the-art of AM biomaterials and technologies but to also critically assess the limitations and challenges that need to be overcome to speed up the clinical adoption of AM vascular stents with both anatomical superiority and mechanical and biological functionalities that exceed those of the currently available mass-produced devices.

2. Stent biomaterials

Vascular stents have undergone three development stages: bare metal stents (BMS), drug eluting stents (DES), and bioresorbable stents (BRS) (Fig. 2) [18]. The first coronary artery stent implanted into a human was a BMS type. BMS were mostly made of stainless steel and cobalt-chromium alloys throughout the 1980s and 1990s. Although these materials could provide robust mechanical support, the initial usage of BMS triggered a number of side effects, such as neointimal hyperplasia [19], which is an inflammatory response to the implanted stent. With implantation time extending, neointimal hyperplasia could cause in-stent restenosis (ISR) and stent thrombosis (ST). To address these clinical issues, DES were developed. The first-generation DES were composed of BMS and permanent polymer coatings, delivering anti-mitotic drugs that could inhibit the proliferation of smooth muscle cells (SMCs) [20]. According to many clinical trials [21], DES were associated with significantly reduced ISR rates, as compared to BMS, and were approved by the Food and Drug Administration (FDA) in 2003. However, endothelial regeneration and vasomotion were impaired, which increased the occurrence of late ST [18]. The development of the second-generation DES was targeting more biocompatible and biodegradable polymer carriers [22]. Nonetheless, since the backbone material of DES stays inside the blood vessel permanently, long-term chronic inflammation and very late ST remain serious concerns [23]. BRS emerged to address the issues associated with the conventional BMS and DES. The main advantage of BRS lies in that the stent can provide mechanical support at an early stage and be absorbed gradually within 1 - 2 years, thereby reducing or even eliminating such adverse effects as ISR and ST [24]. Furthermore, the scaffolding effect exerted by the stent on the blood vessel are deemed unnecessary after the first 6 - 12 months during which arterial remodeling and healing is achieved [25]. Biodegradable metals, made of Mg, Zn, or Fe, and biodegradable polymers, such as polylactic acid (PLA), are the appropriate candidate materials for BRS [26]. This section discusses three types of biomaterials used for vascular stents, including bio-inert metals, biodegradable metals, and biodegradable polymers, and presents their pros and cons.

2.1. Bio-inert metals

Stainless steels (SS) are iron-based alloys containing at least 12% chromium, which are resistant to corrosion in relatively benign environments [27,28]. SS were the first metallic materials used in BMS due to their stable properties, including high strength, good biocompatibility, high degree of corrosion resistance, and low costs. Based on their microstructures, SS can be classified into several families, including ferritic SS, austenitic SS, martensitic SS, and duplex SS [29], each of which has distinct properties. For example, austenitic SS are non-magnetic and, thus, compatible with magnetic resonance imaging (MRI) [30], while ferritic and martensitic SS are ferromagnetic. Moreover, austenitic SS exhibit better corrosion resistance as compared to other categories of SS, rendering them suitable for long-term use in biomedical implants. 316L is a low-carbon version of 316 SS and belongs to austenitic SS. It is widely used for bone plates, screws, and vascular stents [31]. However, 316L may inevitably release harmful metallic ions, such as nickel or chromium ions, due to wear or corrosion. To avoid these negative effects, nitrogen has been used to replace nickel to simultaneously improve the mechanical properties and corrosion resistance of 316L [32].

Cobalt-based alloys were used in medical implants for the first time in the 1930s [28]. Cobalt-chromium (Co-Cr) alloys exhibit better corrosion and wear resistance, as well as higher yield strength and elastic modulus than SS [33,34]. In addition to chromium, molybdenum, tungsten, or nickel are added to cobalt at different concentrations to tune the mechanical properties of Co-Cr alloys. Similar to SS, there are also concerns about the inflammation caused by the release of alloying elements from Co-Cr alloys [35]. Despite their limitations, Co-Cr alloys have been extensively used

Table 1
Commonly used permanent and bioresorbable materials for the development of AM vascular stents and their properties.

Material	Tensile Strength(MPa)	Young's Modulus(GPa)	Elongation (%)	*In vivo* Degradation	Density(g/cm^3)	Biocompatibility
Stainless Steel [28]	540-1000	200	10-40	-	7.9	Ni or Cr may be harmful
CoCr [34]	900-1540	240	2-20	-	9.2	Cr may be harmful
Ta [39]	220-1400	186	2-50	-	16.6	excellent
NiTi [45]	1355	30-50	2-30	-	6.5	Ni may be harmful
Mg alloy [52]	100-300	40-45	2-30	100-4100(μm/y)	1.7	excellent
Fe alloy [61]	200-1000	207	2-60	no obvious weight loss	7.8	good
Zn alloy [71]	20-600	97	1-60	8-120(μm/y)	7.1	good
PLLA [76]	60-70	2-4	2-6	>24 months	1.25	good
PDLLA [76]	40	1-3.5	1-2	3-4 months	1.26	good
PGA [76]	90-110	6-7	1-2	4-6 months	1.53	good
PLGA [76]	65	3.3-3.5	2-6	12-18 months	1.34	good
PCL [76]	23	0.34-0.36	4000	24-36 months	1.15	good

as the backbone materials for DES [36]. Given the high mechanical properties of their underlying alloys, Co-Cr stents can be fabricated with thinner struts (*i.e.*, as fine as 60 - 80 μm [37]) and offer better flexibility than SS stents, leading to lower rates of ST. In addition, the higher density of Co-Cr alloys as compared to SS makes them more radio opaque. This facilitates the positioning of Co-Cr stents in blood vessels and decreases the risk of complications during percutaneous coronary interventions (PCI).

Tantalum (Ta) is one of the refractory materials, which offers high degrees of biocompatibility, corrosion resistance, wear resistance, radio-opacity, and mechanical properties [38,39]. Ta has been employed in dental and orthopedic devices since the 1940s [40]. For example, porous Ta used as bone substitutes has been found to enhance bony ingrowth [41]. The study on Ta as a stent material started in the 1990s [42]. Unlike most other metallic biomaterials, Ta has a negative electrical charge on the surface. This makes Ta highly compatible with blood, because negative electrical charges suppress the formation of thrombi. However, several studies have found that Ta does not significantly reduce the risk of stent-related thrombosis, as compared to SS [43]. Moreover, Ta stents are reported to suffer from poor radial mechanical properties that cause stent recoil after deployment [1]. For these reasons, Ta is currently not studied as a stent material.

Nitinol (NiTi) is an alloy containing an equal amount of nickel and titanium by atomic percentage. It has a low elastic modulus (30 - 50 GPa) but a high compressive strength (1355 MPa), as compared to SS, Co-Cr alloys, and Ta (Table 1). It also exhibits good corrosion resistance and biocompatibility, making it a candidate biomaterial for many biomedical applications [44,45]. More importantly, nitinol shows the shape memory effect and superelasticity, because of martensitic transformation. Since the 1970s, NiTi has been intensively developed for biomedical applications, such as orthodontic wires or braces, bone plates, rods, and screws [46]. Vascular stents made from NiTi tend to be self-expandable, meaning that no balloons are needed to deploy them. The first self-expandable nitinol coil stent was developed in 1983 [47]. The shape memory effect of nitinol allows the stent to self-expand when heated to the body temperature. Self-expandable stents offer better clinical outcomes as compared to balloon-expanded ones, because the superelastic nitinol expands more uniformly and gently [48]. However, nickel is associated with allergic and carcinogenic effects [49]. Therefore, there are concerns regarding the toxicity of nickel-containing implants over long implantation periods [49].

2.2. Biodegradable metals

Magnesium (Mg) is the most developed biodegradable metal due to its good mechanical properties, biocompatibility, and biodegradability [50]. Mg and its alloys have higher strengths (up to 300 MPa) than polymers and lower elastic modulus (40 GPa) than bio-inert metals [51]. It is an essential mineral for a healthy human body, with a recommended daily intake dose of 240 - 420 mg for adults [52]. More importantly, Mg can degrade in physiological environments *via* the formation of magnesium (hydr)oxide and hydrogen. The intermediate biodegradation products can be either absorbed or metabolized in the body fluids. However, Mg has a relatively low standard electrode potential (-2.372 V), causing it to degrade too fast, which may cause early failure of the implant. Intrinsically, Mg has a low ductility at normal body temperature, because of a small number of independent slip systems in its hexagonal close packed (HCP) crystal structure. It can, therefore, not withstand the large deformations that stents experience during their crimping and deployment. Surface treatment [53], alloying [54], and fabrication process optimization [55] have been adopted as the viable strategies to address these issues, in addition to stent design modifications [56,57]. Mg was first used for cardiovascular applications in 1878 when Huse used a Mg wire ligature to stop bleeding vessels [58]. In the last decades, many *in vivo* studies have been conducted on biodegradable Mg stents [59]. The first commercialized Mg BDS received CE marking in Europe in 2016 [60].

Iron (Fe) and its alloys have better mechanical properties, higher radio-opacity, and lower degradation rates than Mg and its alloys. Fe is an essential element for the human body and plays significant physiological roles, making it another appropriate candidate material for biodegradable implantable medical devices [61]. The recommended daily intake dose of Fe for adults is between 8 and 18 mg. Fe can degrade in the body fluid through an electrochemical process involving oxygen absorption without the generation of hydrogen. It shows a low hemolysis ratio, good antiplatelet adhesion ability, and outstanding anticoagulant property [62]. No inflammation or local toxicity was found *in vivo* for pure Fe [63], although the discussion regarding its *in vitro* cytotoxicity remains unsettled. Despite the advantages offered by Fe, it has some disadvantages, including a very low rate of biodegradation and the ferromagnetic nature. Therefore, alloying elements, such as Mn, Pd, Si, and C, have been added to Fe to increase its rate of biodegradation and reduce its magnetic susceptibility [64]. The first biodegradable Fe stent was implanted in the descending aorta of New Zealand white rabbits in 2001 [65]. Lately, the results obtained from several other early pre-clinical studies on Fe-based alloy stents have been promising for future vascular stent developments [66,67].

Zinc (Zn) is considered another promising biodegradable metal for medical applications. The biodegradation rate of Zn is moderate, falling between those of Mg and Fe [68]. Zn is a trace mineral in the human body and plays a crucial role in the immune and nervous systems [69]. The recommend daily intake dose of Zn for adults is between 4 and 14 mg [70]. Although the mechanical properties of pure Zn are relatively low, its intrinsically low degradation rate provides enough freedom for adding non-toxic elements or optimizing processing conditions to improve

its strength and ductility [71]. In 2013, pure Zn wires were implanted into the abdominal aorta of adult male rats for up to 6 months, demonstrating the suitability of Zn as an promising candidate for stent applications [72]. Since then, there have been an increasing number of studies exploring the potential of Zn alloys in various biomedical applications, such as biodegradable vascular stents, orthopedic implants, drug delivery system, and wound-healing agents [73]. In more recent *in vivo* studies, zinc-based alloy stents have been shown to provide sufficient structural support and exhibit appropriate biodegradation rates during long-term implantations without accumulation of biodegradation products, thrombosis, or inflammatory responses [74]. Nevertheless, further investigations are needed to develop biodegradable Zn-based alloys with proper compositions, achieving good biocompatibility, prolonged mechanical integrity, and controlled biodegradation rates.

2.3. Bioresorbable polymers

Bioresorbable polymers under investigation for stent applications include aliphatic polyesters, polyorthoesters, and polyanhydrides, among which aliphatic polyesters are the most frequently used materials for bioresorbable stents [75,76]. Poly-L-lactic acid (PLLA), poly-D, L-lactic acid (PDLLA), poly ε-caprolactone (PCL), polyglycolic acid (PGA), and poly (lactic-co-glycolic acid) (PLGA) are all aliphatic polyesters. The raw materials of bioresorbable polymers are normally in the form of filament, powder, or resin. For photopolymerization, polyesters need to be further functionalized with photocrosslinkable groups. In addition, other components, such as photoinitiators, diluents, dyes, and radical inhibitors, are added to adjust the properties of the resin [77]. Normally, the polymers in the poly-lactic acid (PLA) family, such as PLLA and PDLLA, have relatively high tensile strengths and low rates of biodegradation, while PCL and PGA have lower tensile strengths and higher rates of biodegradation. Since PLGA is a co-polymer composed of PLA and PGA, its physicochemical properties can be controlled by changing the molar ratio of lactic acid and glycolic acid in the polymer chains [78]. These polymeric biomaterials can degrade through the hydrolysis of the ester bond in the polymer backbone. Through partial chain scission, biodegradable polymers can degrade into 10 - 40 μm particles, which can be phagocytosed and metabolized to resorbable carbon dioxide and water [79]. The degradation time of such polymers is dependent on a number of internal factors, such as their chemical structures and molecular weights, as well as several external factors, including pH, temperature, and the presence of bacteria or inorganic fillers [80]. So far, polylactide (PLA) has been the most common bioresorbable material for BRS due to its high biocompatibility, biodegradability, good processability, and good mechanical properties. However, several limitations of PLA stents have been recognized, including the lack of radio-opacity, poor toughness, and low radial mechanical properties [81]. Therefore, the strut thickness of PLA stents needs to be greater, which may cause higher rates of adverse events, such as neointimal hyperplasia, vessel recoil, and ST. Optimization of material processing conditions and molecular orientations as well as the application of thermal annealing have been reported to be the most successful strategies for the enhancement of the mechanical performance of polymeric stents [82,83].

3. Additive manufacturing technologies and post processing

AM is a layer-by-layer manufacturing approach that is fundamentally different from the traditional (subtractive) manufacturing processes. AM provides unprecedented opportunities to tackle the dilemma between freeform design and manufacturability [84]. Over the last 30 years, AM technologies have tremendously advanced. Nowadays, AM allows for precise manufacturing of complex, composite, and hybrid structures as well as functionally graded materials (FGMs) [85]. It is able to produce fully functional parts made from a wide range of materials, including metals, ceramics, polymers, and their combinations. According to the International Organization for Standardization (ISO)/American Society for Testing and Materials (ASTM) 52900:2015 standard, AM technologies can be classified into seven categories: binder jetting (BJ), directed energy deposition (DED), material extrusion (ME), material jetting (MJ), powder bed fusion (PBF), sheet lamination (SL), and vat photopolymerization (VP) [86]. Specific AM technologies are linked to certain types, forms, and physical states of materials. For example, DED works with metallic powders or wires as the feedstock material, is limited in terms of the minimum feature size and surface quality, and is more suitable for fabricating larger components. SL bonds sheets of materials to form objects and is limited in the geometrical complexity it can achieve. DED and SL technologies are, therefore, not suitable for fabricating delicate stents and are not included in this review.

3.1. Powder bed fusion

PBF AM techniques uses either laser or electron beams to selectively melt or fuse powder particles on a powder bed and in layer-by-layer manner. PBF can be further categorized into selective laser sintering (SLS), laser-based powder bed fusion (LB-PBF), and electron beam powder bed fusion (EB-PBF). The main difference between SLS and LB-PBF lies in whether the source of energy totally melts powder particles (LB-PBF) or merely fuses them together (SLS) (Fig. 3**a**). SLS is primarily applied to polymers while LB-PBF and EBM are chiefly direct metal AM techniques. We did not find any reports in the literature regarding the application of EBM to vascular stents, likely due to the larger spot sizes of electron beams (~100 μm) as compared to those of laser beams (~50 μm).

3.1.1. Laser-based powder bed fusion

In 2017, Demir *et al.* [87] produced CoCr cardiovascular stents through LB-PBF using a pulsed-wave laser. The geometrical fidelity of the resulting stents appeared to be highly dependent on the scanning strategy, laser peak power, and pulse duration. It was found that concentric scanning was more suitable for fabricating fine struts as compared to hatch scanning. Increasing the peak laser power and pulse duration enlarged the strut thickness but reduced the surface roughness. Surface quality was improved when loosely adhered particles were removed through post-LB-PBF electrochemical polishing (Fig. 3**c**). Finazzi *et al.* [88] defined a number of design rules for producing expandable stents, including part orientation, strut inclination, and strut overhangs. For example, length of the strut overhangs was suggested to be < 1 mm while spacing should be > 0.3 mm. Based on these rules, CoCr tubular semi-crimped stents were fabricated and were successfully expanded without cracks or breakage. The researchers further demonstrated bifurcated designs realized by LB-PBF. The stents showed sufficient flexibility at their connection sites to allow for the deformations leading to the desired final shape (Fig. 3**b**). In a follow-up study, the same group designed, fabricated, polished, and functionally tested a type of CoCr stents [89]. Stent samples were tested under different pressures to determine their expandability. The results showed that both the external diameter and expansion ratio increased with the applied pressure, without any cracks (Fig. 3**g**). Omar *et al.* [90] evaluated 7 types of stent designs, all made with LB-PBF from a medical grade CoCr powder. They also defined the processibility window for AM of stents. The average densities of the struts of these 7 stents were between 92 and 97%.

In addition to CoCr, 316L SS stents have been fabricated with LB-PBF. Langi *et al.* [91] compared an LB-PBF 316L SS tube (with

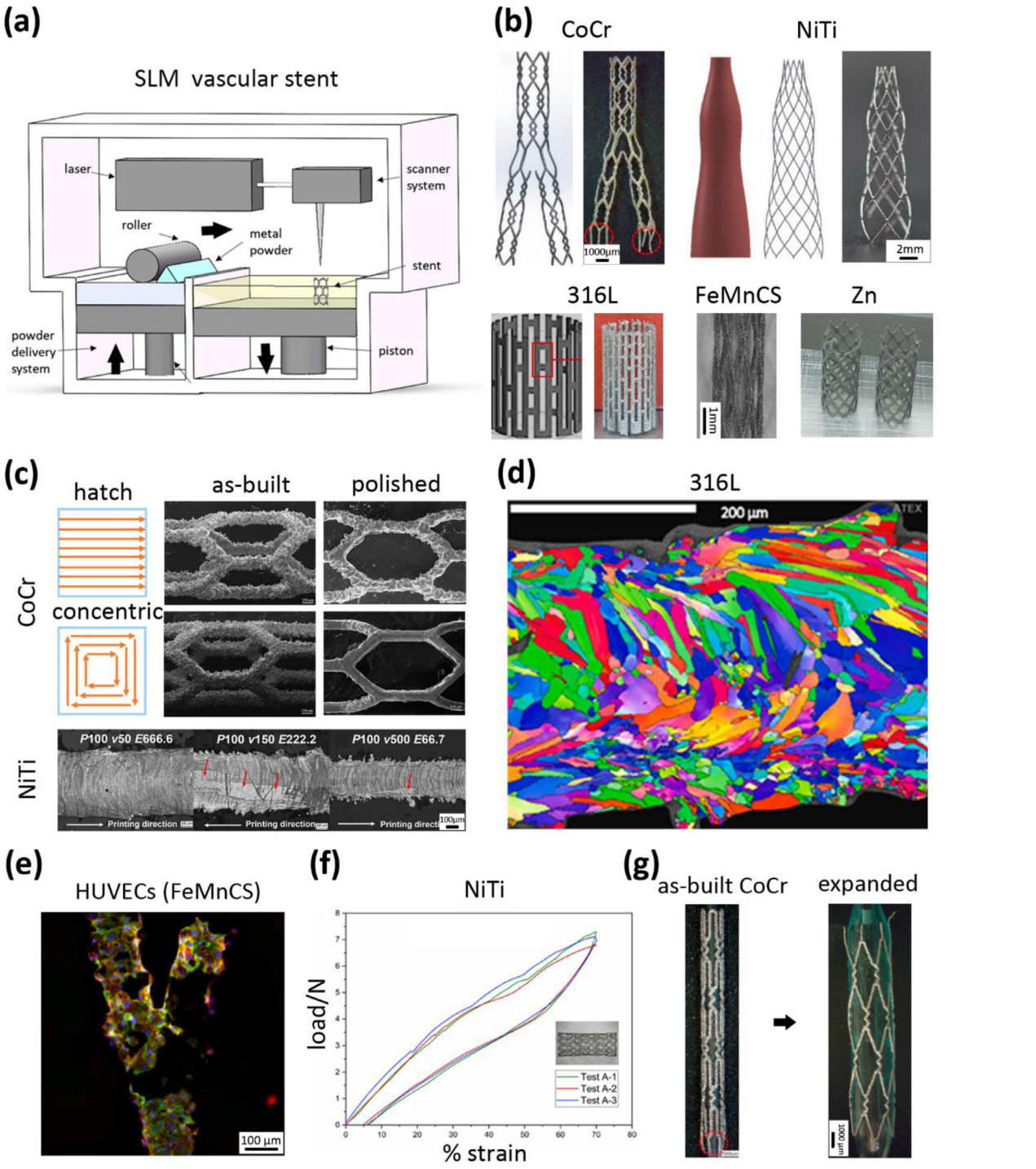

Fig. 3. LB-PBF vascular stents: (a) a schematic illustration of the LB-PBF process, (b) LB-PBF metallic stents [89,92,95,103], (c) the effects of LB-PBF process parameters and post-AM treatments on the morphology of LB-PBF CoCr stents and NiTi stents [87,94], (d) the microstructures of LB-PBF 316L stents [92], (e) fluorescence image of HUVECs seeded on LB-PBF FeMnCS stents and cultured for 7 days [103], (f) the superelasticity of LB-PBF NiTi stents [94], and (g) an expansion test of LB-PBF CoCr stents [89] .

a wall thickness of 150 μm) with a commercial stent. The LB-PBF specimens had columnar and coarse grains, as opposed to the equiaxed and fine grains in the commercial stent. The chemical composition of LB-PBF 316L SS was similar to that of the commercial stent, confirming little element loss during the LB-PBF process. Subsequently, the same group of researchers printed a 316L SS stent with a strut thickness of 360 μm (Fig. 3**b**) [92]. The microstructure of the LB-PBF stents was composed of a cellular subgrain structure and a columnar grain structure, as revealed by electron back-scattered diffraction (EBSD) (Fig. 3**d**). The hardness values and elastic moduli of the LB-PBF stents were higher than those of the commercial one. However, the LB-PBF stent showed high degrees of anisotropy in its elastic modulus and hardness. Chen *et al.* [93] designed and fabricated anti-tetrachiral auxetic 316L SS stents with negative Poisson's ratios using LB-PBF. They used the diameters of the circular node to tune the Poisson's ratio of the stents. These LB-PBF 316L SS stents showed good biocompatibility when in contact with human umbilical vein endothelial cells (HUVECs). However, the wall thickness of the stents appeared to be quite large (0.6 – 1.5 mm).

Nitinol can be used for self-expandable stents due to its superelasticity and shape memory effect. Yan *et al.* [94] investigated the process-microstructure-property relationships of nitinol wires and 3D printed nitinol stents with two closed-cell designs (Fig. 3**c**). The LB-PBF nitinol stents showed a high strut density, a uniform strut diameter (200 µm), adequate superelasticity (Fig. 3**f**), and high compatibility with sarcoma osteogenic (SAOS2) cells. Both stents were loaded to reach a 70% displacement and the non-recoverable strain was found to be only 4 - 6%. Finazzi *et al.* [95] proposed a framework for developing patient-specific nitinol stents fabricated by LB-PBF. They designed personalized stents (with a strut thickness of 100 µm) with varied diameters adapted to match dimensions of patients' vessels. It was demonstrated that LB-PBF nitinol stents with designed geometries could be produced with high fidelity and that structural details could be preserved (Fig. 3**b**). Jamshidi *et al.* [96] studied the effects of laser energy during LB-PBF on the characteristics of nitinol stents. The nitinol microstructure was composed of large plates and some irregular smaller plates, indicating the presence of both martensite and austenite phases. They found that the austenite finish temperature was strongly dependent on the Ni concentration in the alloy. In addition, the LB-PBF nitinol stents exhibited an elastic modulus (56 - 73 GPa) which was comparable with that of a conventionally fabricated austenitic NiTi. Chemical etching after LB-PBF not only removed the unmolten powder particles but also reduced the strut size.

While several LB-PBF Ta scaffolds have been developed for orthopedic applications, no LB-PBF Ta stent has been reported in the literature [97]. Similarly, while LB-PBF biodegradable metallic bone implants have been intensively developed recently [98–102], very limited information can be found regarding LB-PBF biodegradable metallic stents. In 2022, Paul *et al.* [103] have reported successful LB-PBF-based manufacturing of a biodegradable Fe-30Mn-1C-0.02S stent with a dimeter of 2 mm, a length of 13 mm, and a strut thickness of 120 µm (Fig. 3**b**). The as-built stents had fine grain sizes (18 $\pm$ 2 µm) within the struts and at the junctions (30 $\pm$ 4 µm). The Fe stents exhibited mechanical properties that were comparable with those of a commercial 316L SS stent. *In vitro* biodegradation tests of these stents showed that the release of iron and manganese ions increases from 0.22 µg/mL and 0.15 µg/mL after 2 hours to 0.42 µg/mL and 0.35 µg/mL after 28 days, respectively. The LB-PBF iron stents also exhibited good cytocompatibility when brought in direct contact with HUVECs for 7 days (Fig. 3**e**). Given that LB-PBF biodegradable Mg and Zn bone scaffolds with strut thicknesses between 200 and 500 µm have been successfully manufactured with good manufacturing fidelity and biocompatibility [104–107], it is expected that LB-PBF Mg and Zn stents could be developed for further investigations. Indeed, the first LB-PBF Zn stent prototypes have been recently developed (Fig. 3**b**) and are being subjected to characterization and evaluation.

Currently, LB-PBF metallic stents are still in their infancy and most of the available reports concern proof-of-concept studies that are designed to explore and understand their manufacturability, printing accuracy, microstructural features, basic mechanical properties, and *in vitro* cytocompatibility. The complete *in vitro and in vivo* functional tests, including radial strength, elastic recoil, and fatigue resistance, as well as investigations of the post-AM processes for surface enhancement and related hemocompatibility are yet to be performed.

3.1.2. Selective laser sintering

In 2013, Flege *et al.* [108] used polymer laser sintering (pLS) – a subdivision of SLS that may exceed the melting temperature of the polymer but stays below its deterioration temperature [109,110] – to build coronary stent prototypes from PLLA and PCL powders. After optimizing the laser power, laser beam diameter, powder layer thickness, and deposition speed, stent prototypes with a wall thickness of 180 - 200 µm were successfully manufactured, showing no pores on their cross-sections (Fig. 4**a**). Although the as-built stents had a very rough and uneven surface, it could be smoothened by applying spraying or dip-coating or a combination thereof (Fig. 4**b**). Both SLS polymers showed good direct and indirect biocompatibility with human arterial smooth muscle cells (haSMCs), HUVECs, and endothelial progenitor cells (EPCs) (Fig. 4**c**). Initially, a simple stent prototype with rhombic cells was developed, which was expandable with a conventional balloon. Subsequently, the radial strength and expandability of the stent were improved by using longer and rounder cells. Moreover, a cone-shaped stent with a continuous strut configuration in the linking region for bifurcation applications was demonstrated through SLS (Fig. 4**a**). In 2018, Geng *et al.* [111] used SLS to fabricate an auxetic cylindrical stent from a nylon powder (Fig. 4**a**). Since arterial endothelium has a negative Poisson's ratio [111], an auxetic stent may better match the native blood vessel tissue, thereby reducing deformation incompatibility. The proposed chiral stent exhibited auxetic behavior and could be tailored by adjusting the design parameters of the unit cell. Studies on SLS stents are, however, quite rare and no *in vivo* tests have yet been carried out. In general, SLS offers resolutions that are close to the ones required for reaching the desired thickness of the struts within the stent, can incorporate drugs into the polymer matrix, and is suitable for building specially shaped stents for bifurcation applications. Further systematic investigations on biodegradation, biocompatibility, and stent recoil need to be performed in the future.

3.2. Binder jetting

BJ is an AM method in which powder particles are spread into a layer and selectively joined into the designed 2D shape with a liquid binder (Fig. 5**a**) [112]. As the process progresses, the 2D layers bound together, resulting in the desired 3D geometry. The printed parts will then be subjected to post-AM treatments, typically including curing and depowdering to create "green" parts, followed by sintering to achieve good mechanical properties. BJ has been applied to develop many ceramics, metals, and composites for orthopedic or pharmaceutical applications (Fig. 5**b**) [113–117]. However, no literature on BJ stents was found. In principle, BJ can be used to print metallic vascular stents (Fig. 5**a**). The main challenge lies in minimizing internal pores in the struts and controlling the shrinkage of the BJ stent during sintering.

3.3. Material jetting

MJ typically uses multiple nozzles to deposit droplets of both base and support materials [118]. After each layer is deposited, curing with ultraviolet (UV) light takes place to harden the deposited layers (Fig. 6**a**). After printing, the support material can be dissolved to obtain the final object. The main advantage of MJ lies in its ability to combine different materials. Moore *et al.* [119] used a poly-jet MJ printer to build poly-propylene stents with a range of diameters (4 - 10 mm) and a strut thickness of 300 µm (Fig. 6**b**). The actual thickness of the printed stents was, however, higher (about 400 µm), because the applied large-scale printer with a limited resolution was not really suitable for printing such small stents. Expansion tests were carried out and the stents failed due to the linear delamination along the vertical axis. Xue *et al.* [120] designed a self-expanding auxetic stent and fabricated a 15-times larger version through MJ (Fig. 6**b**). However, this approach is only suitable for prototyping and the material used was a combination of commercially available polymers (*i.e.*, 30% Vero and 70% Tango) with unknown degree of biocompatibility. Biocompatible MJ

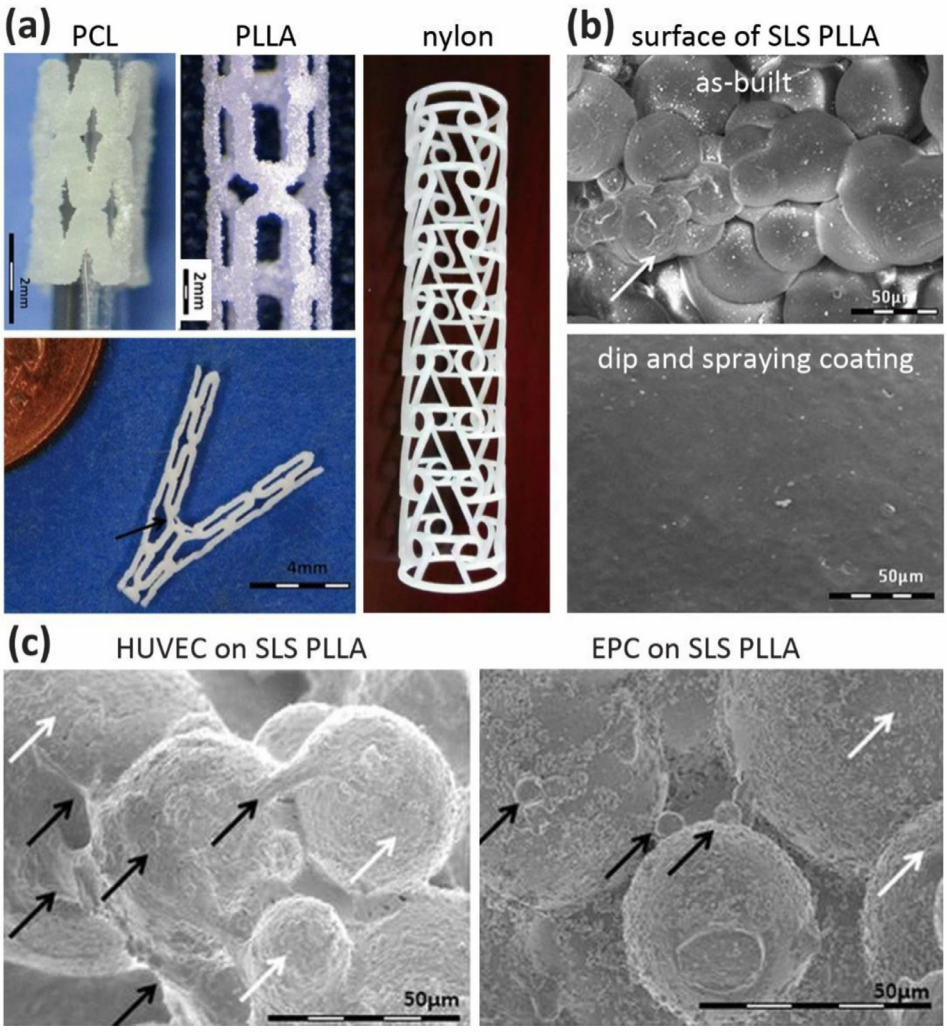

Fig. 4. SLS vascular stents: (a) SLS polymer stents [108,111], (b) surface modification of SLS PPLA stent by applying dip-coating and spray-coating [108], and (c) the direct biocompatibility tests of HUVEC and EPC on SLS polymer stents [108].

feedstock materials with low viscosity and better final mechanical properties need to be developed for MJ stents in the future.

3.4. Materials extrusion

Fused deposition modeling (FDM) and direct ink writing (DIW) are the two common AM techniques that operate under the principles of ME. During FDM, a filament is fed into a heated extrusion head and the filament material is deposited in layer-by-layer fashion (Fig. 7**a**). A wide variety of thermoplastics are suitable for FDM, including PLA, PLGA, and PLC [121]. During DIW, a viscoelastic ink is extruded at or moderately above room temperature, followed by solidification through different mechanisms, such as UV radiation, solvent evaporation, or sintering [122]. Therefore, many more types of materials can be printed with DIW, including curable resin-based materials similar to SLA and DLP. So far, FDM has been the most commonly used AM technique to develop AM vascular stents.

3.4.1. Fused deposition modeling

In 2017, Cabrera *et al.* [123] used an FDM printer to print a bioresorbable thermoplastic copolyester (TPC) elastomer stent (Fig. 7**b**). The 3D printed prototype stents differed from the initial design due to the low resolution of the FDM printing technique. Although the as-built stents had some imperfections within their struts, chemical etching could eliminate extra wires without influencing their performance. The stents were self-expandable and showed a radial strength that was comparable to that of a nitinol stent (Fig. 7**c**). After three weeks of enhanced degradation tests at 90°C, the struts were partially hydrolyzed with pores or cracks on the surface (Fig. 7**d**). The low resolution of the FDM technique was considered to be the main limiting factor that affected the performance of the stent.

Jia *et al.* [124] developed a self-expandable PLA stent through FDM. The stent could be compressed and maintained its shape at room temperature, while recovering to its original shape upon heating to 70 °C (Fig. 7**e**). In a different study, Wu *et al.* [125] investigated the shape memory effect of FDM PLA stents and found that the recovery ratio could reach as high as 95% at 65 °C (Fig. 7**e**).

FDM stents typically have some limitations, such as stair-stepping on the surface, mechanical anisotropy, and the need for support when printing designs involving large overhangs [126]. To overcome these limitations, rotating mandrel-assisted AM (RMS-AM) has been developed, in which the feedstock material is extruded on the surface of a rotating cylindrical mandrel (Fig. 8**a**). In 2015, Park *et al.* [127] printed a PCL stent on a rotating shaft by FDM (Fig. 8**b, c**). Sirolimus, mixed with PLGA and polyethylene glycol (PEG), was sprayed on the stent surface to form DES. *In vivo* tests confirmed that the DES could, indeed, reduce neointimal hyperplasia with a desirable (*i.e.*, low) fibrin score in the porcine

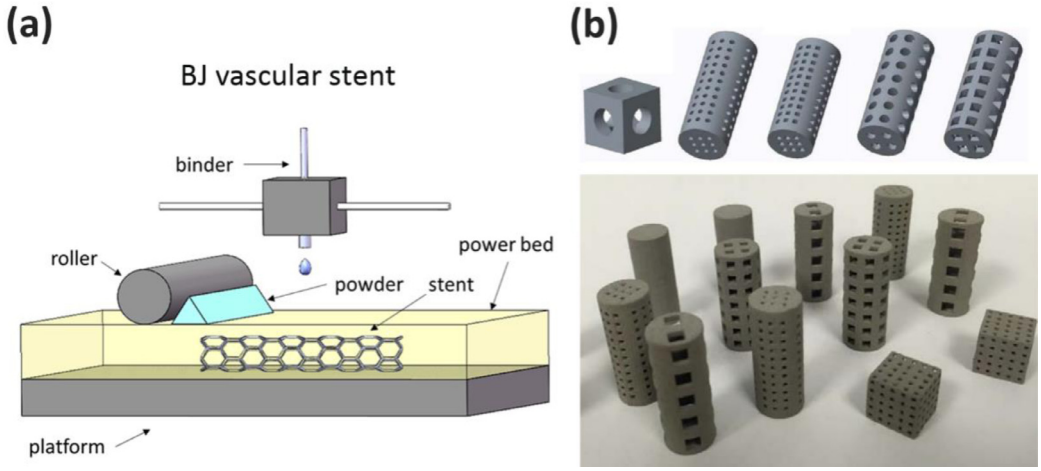

Fig. 5. BJ biomedical implants: (a) a schematic illustration of the BJ process and (b) BJ 316 stainless steel scaffolds [117].

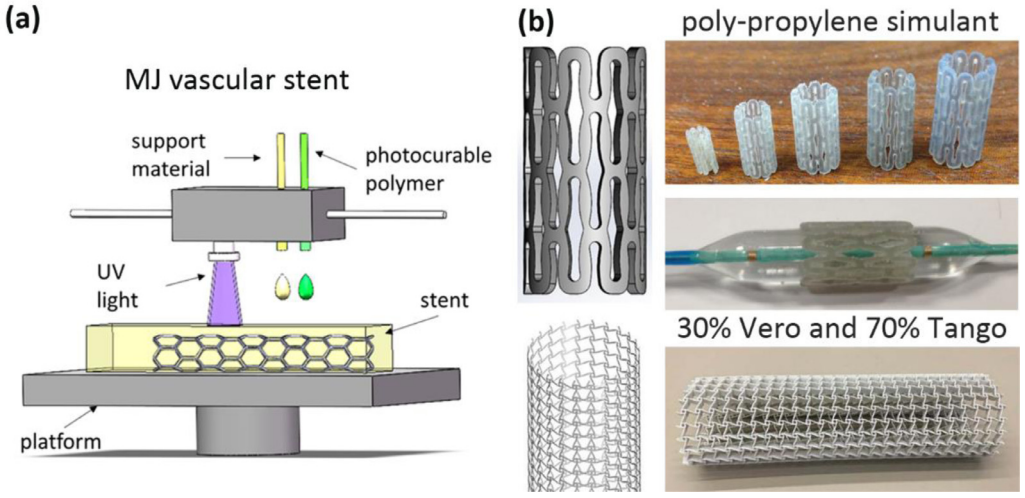

Fig. 6. MJ vascular stents: (a) a schematic illustration of the MJ process and (b) MJ polymer stents [119,120].

femoral artery. Guerra *et al.* [128,129] investigated the effects of printing parameters on the dimensional precision and mechanical properties of RMS-AM PCL stents (Fig. 8**d**) and found the strong influences of printing temperature and flow rate, while printing speed did not exert any influence. The printed stent specimens, with an average expansion ratio of 320% and a recoil ratio of around 22%, showed a good radial behavior. Wang *et al.* [130] developed screw-extrusion-based RMS-AM equipment and fabricated PLLA and PCL stents with different shapes and geometries (Fig. 8**b, c**). The *in vitro* results in terms of the hemolysis rate and cell viability confirmed the potential of the RMS-AM stents for vascular implantation. However, they found that PCL stents were not completely reliable with respect to radial strength and radial recoil. Considering that most of RMS-AM stents have had a relatively large stent thickness (190 - 500 μm), Somszor *et al.* [131] applied melt electrowriting (MEW) that could be used to fabricate composite stents with thin struts (60 - 80 μm) and a high degree of geometric complexity (Fig. 8**b, c**). MEW polycaprolactone-reduced graphene oxide (PCL-rGO) nanocomposite stents were found to have superior mechanical properties as compared to monolithic PCL. The cytocompatibility of the material was not adversely affected either (Fig. 8**e**). In 2022, Shen *et al.* [132] reported personalized, heparinized, and biodegradable coronary artery PCL stents fabricated through RMS-AM (Fig. 8**c**). The printed stents exhibited high compressive properties and good flexibility (Fig. 8**f**). Heparinization reduced the adhesion of platelets, promoted the adhesion and proliferation of endothelial cells (ECs), and inhibited the proliferation of SMCs *in vitro*. The stents showed good biocompatibility and mechanical strengths within 12 weeks and maintained patency without acute thrombosis formation after implantation in rabbit abdominal artery (Fig. 8**g**). Of note, there has already been a clinical trial of RMS-AM PLLA stents (Clinical Trial Protocol, Approval No. 2019L0001, National Medical Products Administration, China) [133] in China.

3.4.2. Direct ink writing

Similar to RMS-AM, DIW relies on a rotating mandrel system to fabricate stents (Fig. 9**a**). Chausse *et al.* [134] dissolved PLLA in chloroform and obtained a viscous, printable polymeric solution. Then, stents with a variety of designs were printed through DIW on a rotating mandrel at room temperature, followed by a thermal treatment at 80 °C for 12 h to ensure complete chloroform evaporation (Fig. 9**b**). The DIW stents exhibited encouraging mechanical and biological properties *in vitro*. Moreover, the ink could be modified by adding iodine, 2,3,5-triiodobenzoic acid (TIBA), or $BaSO_4$ as a radio-opaque agent to obtain the required stent radio-opacity (Fig. 9**c, d**).

Among all the AM techniques applied to fabricate stents, the development of ME stents is at the forefront. This is evidenced by the several *in vivo* pre-clinical studies and one clinical trial performed to date. The main advantage of ME for the development of vascular stents lies in the fact that it is compatible with many FDA

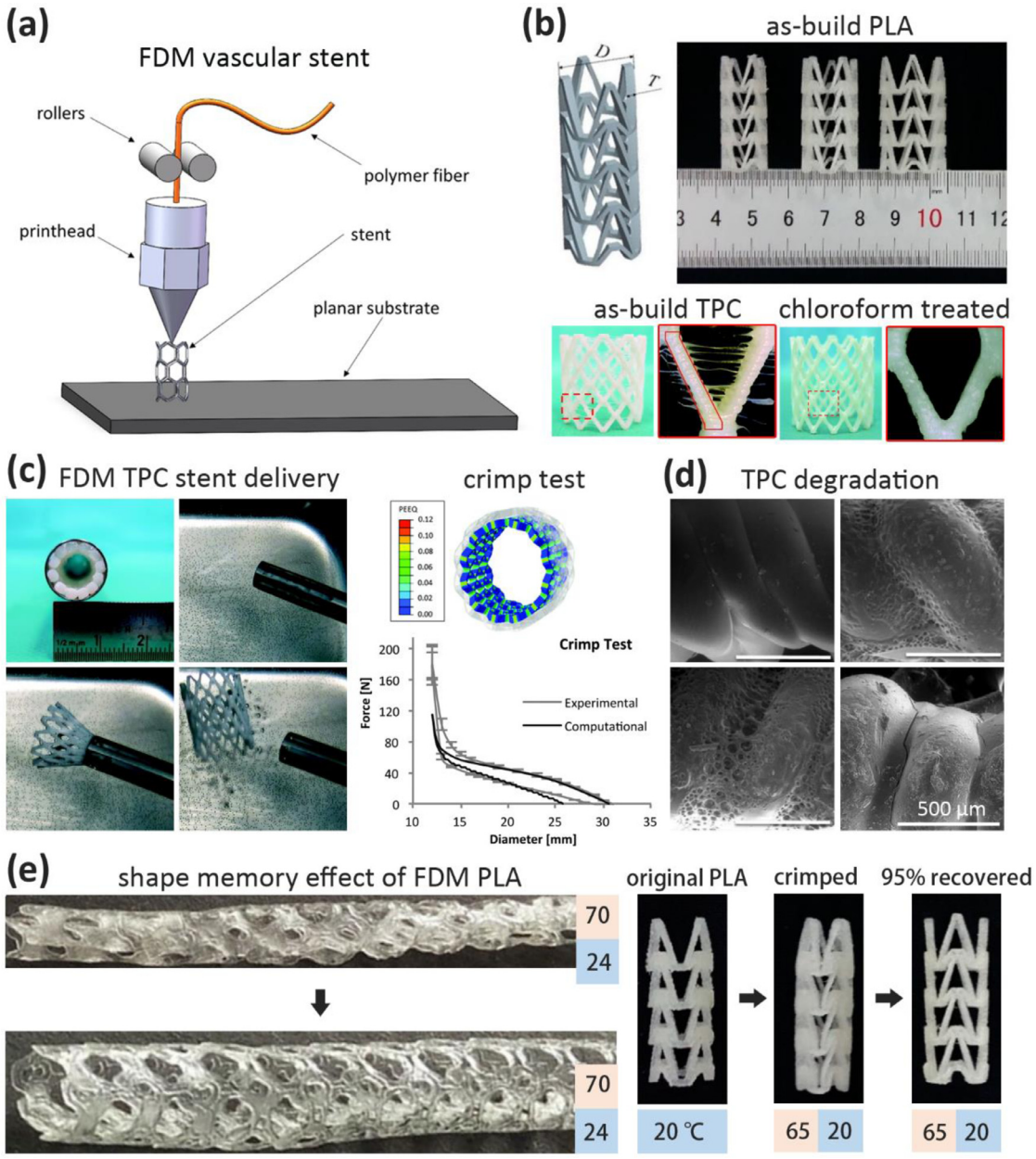

Fig. 7. FDM vascular stents: (a) a schematic illustration of the FDM process, (b) FDM polymer stents and their surface treatment [123,125], (c) the delivery and crimp test of FDM TPC stent [123], (d) the biodegradation of FDM TPC stent [123], and (e) the shape memory effect of FDM PLA stent, orange and blue blocks represent the temperature during deformation and recovery of the stent [124,125].

approved materials, such as PLA and PLC. More materials compatible with FDM or DIW are expected to be developed in the future to fulfil the mechanical and biological requirements of vascular stents.

3.5. Vat photopolymerization

VP is a 3D printing process that makes use of photopolymerization to build solid 3D objects. In this technique, a vat of liquid photopolymer resin is selectively solidified through exposure to UV light. The printing platform then moves downwards to print the next layer. VP technologies includes stereolithography (SLA) and digital light processing (DLP). The UV source of SLA is a laser that hardens the resin point by point, while a DLP printer uses a projected light source to cure the entire layer across the whole platform at once. Within the DLP-based AM, several variants have emerged, such as projection micro stereolithography (PμSL) and continuous liquid interface production microstereolithography (μCLIP). PμSL is capable of printing complex 3D structures with a high resolution (up to 0.6 μm) [135], while μCLIP allows for faster printing (<10% of the printing time needed for PμSL) [135,136]. During the DLP process, the initial polymerization of the resin happens at the bottom of the tank where oxygen supply could be inhibited, leading to incomplete curing and a sticky surface. μCLIP was developed to overcome this problem by introducing an oxygen-permeable window that could form a thin uncured material layer at the top [137]. In addition, the platform of μCLIP moves continuously instead of moving step by step as in the case of DLP, thus eliminating the possibility of delamination between layers (Fig. 10**a**). In addition to resins, VP has also been applied to print metal and ceramic slurries mixed with photopolymers.

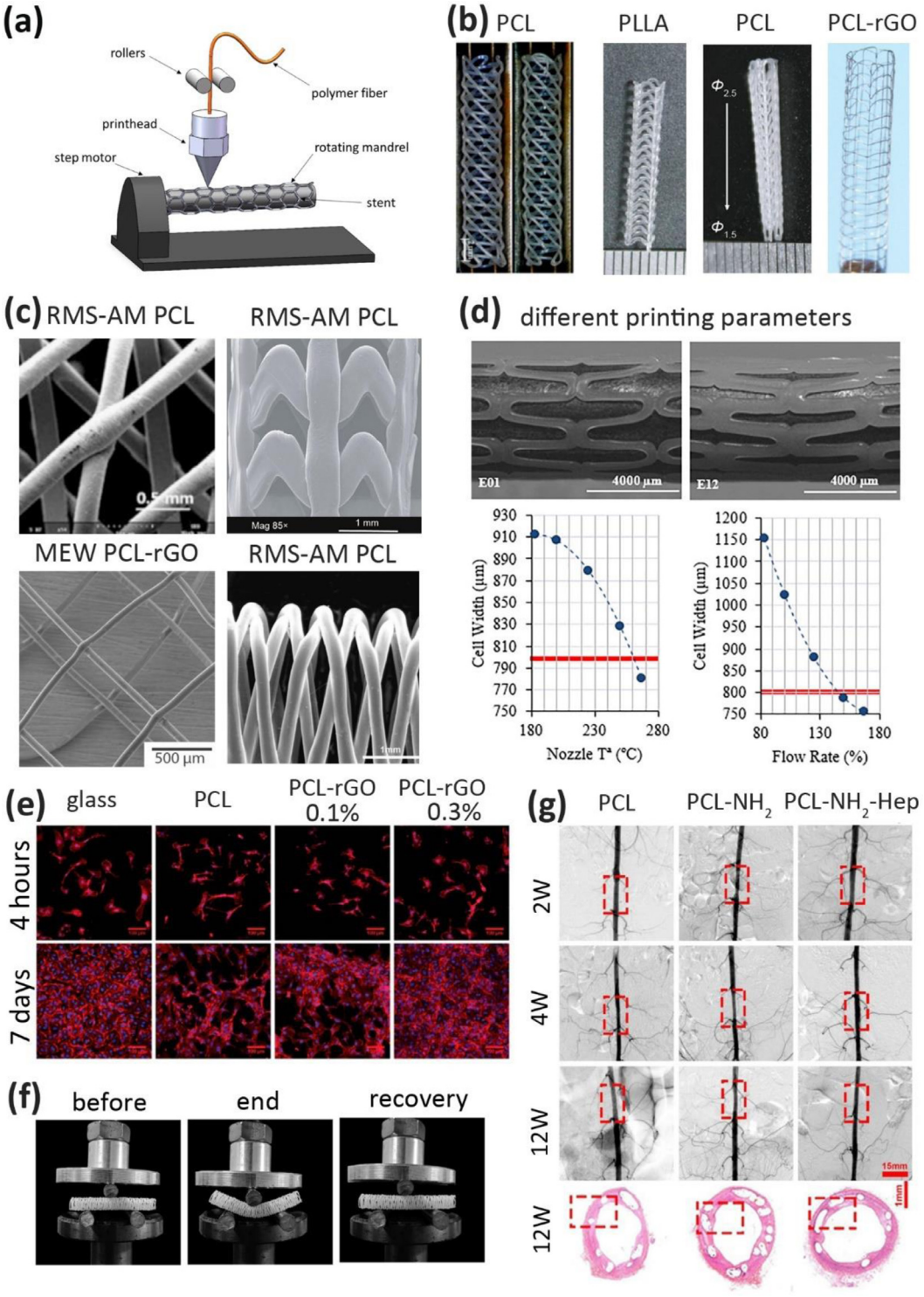

Fig. 8. RMS-AM vascular stents: (a) a schematic illustration of the RMS-AM process, (b) RMS-AM stents [127,130,131], (c) the strut morphologies of RMS-AM stents [127,130-132], (d) the effects of printing parameters on the morphology of RMS-AM PCL stents [128], (e) the biocompatibility of RMS-AM PCL and PCL-rGO stents [131], (f) the three-point bending test of RMS-AM PCL stents [132], and (g) representative angiography images and H&E staining of RMS-AM PCL stents implanted vessels after implantations [132].

In 2016, van Lith *et al.* [138] developed a bioresorbable and antioxidant polymer from methacrylated polydiolcitrate (mPDC) and used it to make a stent *via* μCLIP. The stent achieved a high lateral resolution of 7.1 μm and a layer thickness of 20 μm (Fig. 10**b**). The mechanical properties of the stent were comparable to those of a nitinol stent. The 3D printed stent could self-expand and had a significantly increased radial compression strength after deployment in a pig artery (Fig. 10**c**). Moreover, the stent lost up to 25% of its mass loss after 6 months of biodegradation in phosphate buffered saline (PBS) at 37°C. It also neutralized 100% of the free radicals within 2 weeks. However, the cross-sectional profile of the stent (with a strut thickness of 150 μm and a wall thickness of 500 μm) was considered too large to be used in real clinical cases. In 2018, the same group optimized the μCLIP process and the composition

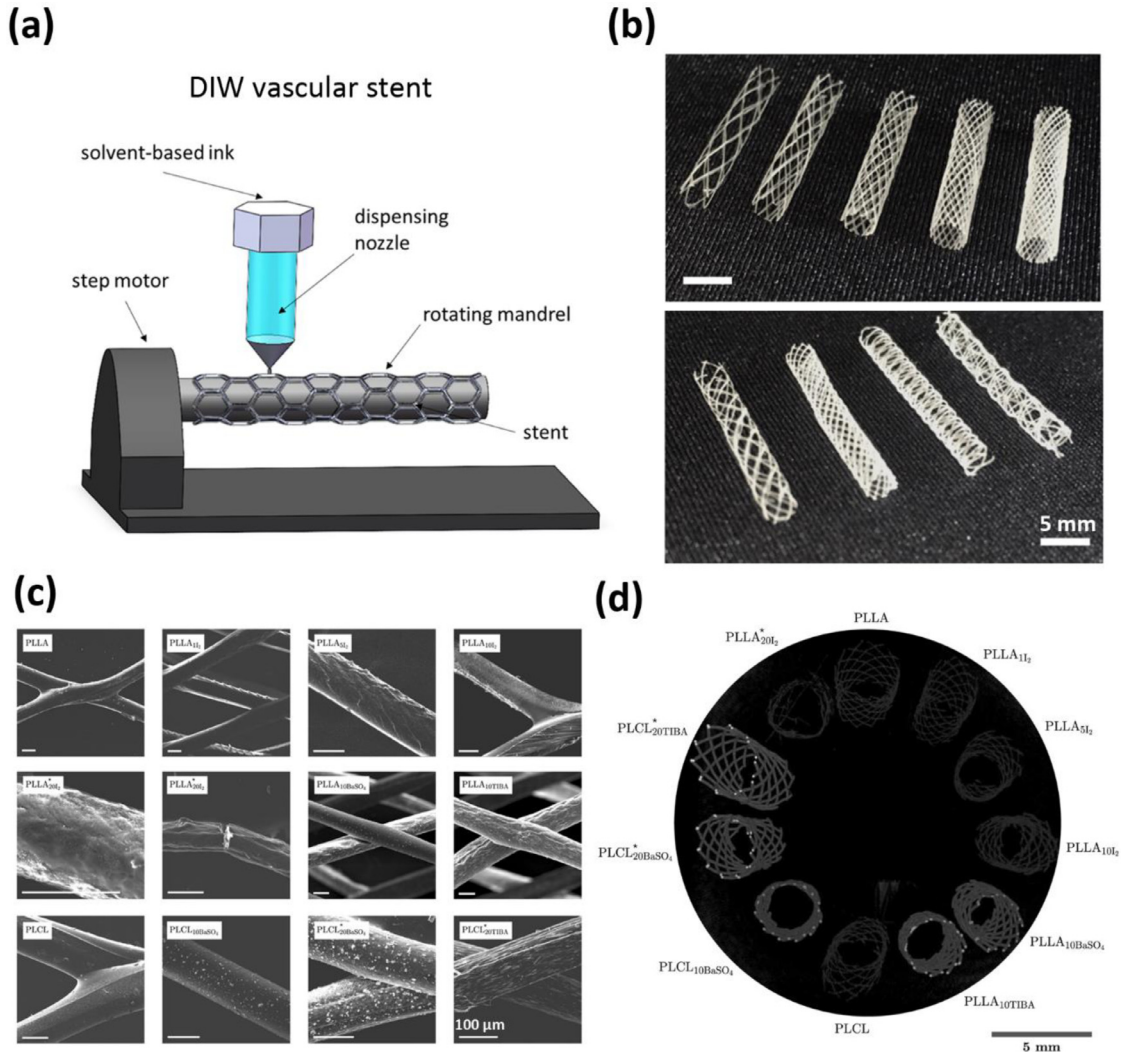

Fig. 9. DIW vascular stents: (a) a schematic illustration of the DIW process, (b) DIW stents [134], (c) the morphologies of DIW stents [134], and (d) the radio-opacity of DIW stents made from different inks [134].

of the citric acid-based bioresorbable ink to maximize the stent radial stiffness (Fig. 10**d**) [139]. The stent was successfully fabricated with a strut thickness of 150 μm and a radial stiffness comparable to those of nitinol stents. The lead time was greatly reduced to 30 minutes for fabricating a 2 cm-long stent. In addition, the stent showed good compatibility with HUVECs *in vitro*.

Recently, DES have been developed through DLP. Oliveira *et al.* [140] incorporated nitric oxide (NO) donor S-nitroso-N-acetyl-d-penicillamine (SNAP) into the mPDC matrix and printed NO-releasing stents through DLP (Fig. 10b). The printed stents exhibited adequate mechanical properties to allow for stent compression and self-expansion. Hydrolytic degradation and NO release were initiated once the stent was in contact with an aqueous medium (*i.e.*, a 0.01 M NaOH solution, pH = 12.0, 60°C) (Fig. 10**e**). The release rate of NO could be controlled by keeping the SNAP charge in a suitable range to inhibit thrombus formation.

In summary, VP can fabricate stents with complex geometries at high resolutions. However, the material used for VP needs to be photocurable, limiting the use of many mature biocompatible polymers, such as PLA, PLGA, and PLC. More photocurable and biocompatible inks need to be developed. Since VP can be also used to print metallic slurries, it may be possible to fabricate metallic stents through VP in the future.

3.6. 4D printing

4D printing concerns the targeted evolution of a 3D printed structure, in terms of shape, property, or functionality upon triggering by a stimulus [141]. 4D printing basically uses the same AM facilities as described above (*e.g.*, LB-PBF, SLA, FDM, DIW, or DLP). The main difference is that the feedstock material in 4D printing may need to possess such properties as self-sensing, decision making, responsiveness, shape memory, self-adaptability, multifunctionality, or self-repair [142]. Since 2016, several researchers have employed 4D printing to develop advanced vascular stents. Most of such studies take advantage of the self-expansion property provided by 4D printing, thereby enabling minimally invasive surgery to treat vascular diseases [143]. For example, Wei *et al.* [144] used DIW for the 4D printing of stents. The stents were made from either a shape memory polymer (SMP) (*i.e.*, PLA) or a shape memory nanocomposite (SMNC) (*i.e.*, PLA-Fe_3O_4). After deformation, both SMP and SMNC stents could recover to their original shapes when heated in water and when exposed to the heating caused by an alternating magnetic field, respectively (Fig. 11**a**). Ge *et al.* [145] developed a photo-curable methacrylate-based copolymer and used it to 4D printed stents through PμSL. The stents were recovered their original shape after heating to 60 °C (Fig. 11**b**). The

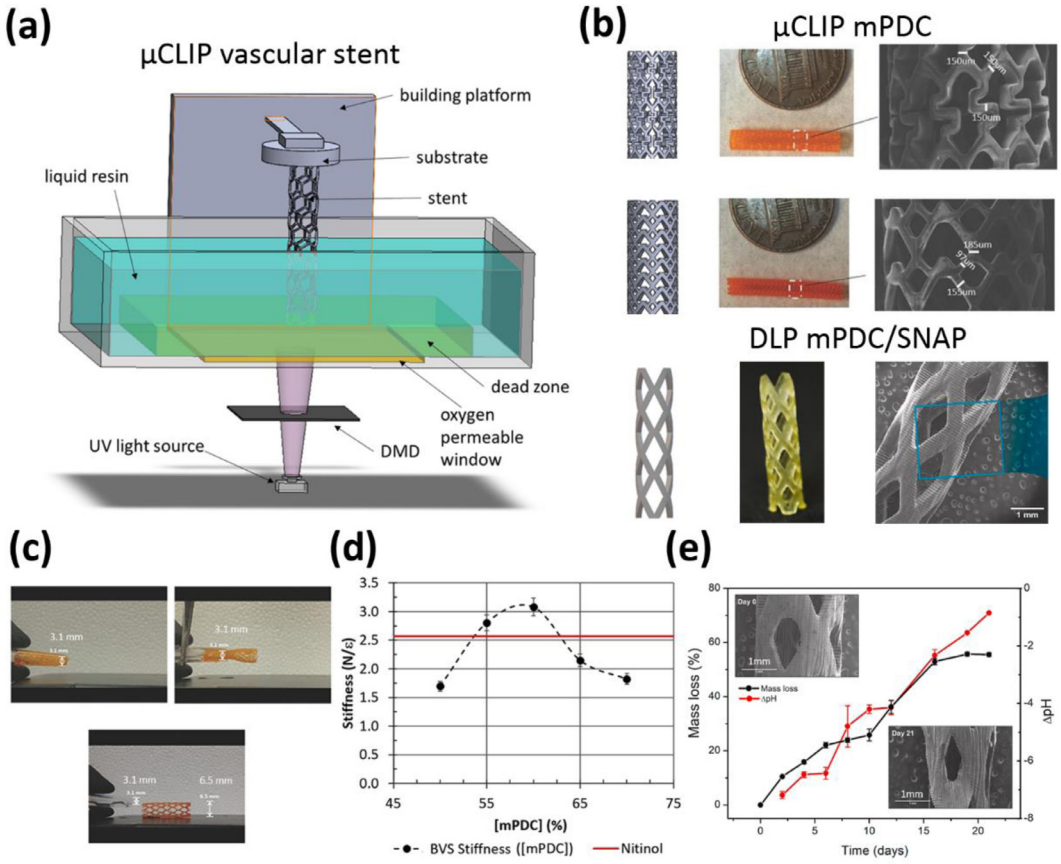

Fig. 10. VP vascular stents: (a) a schematic illustration of the μCLIP process, (b) μCLIP stents [138,140], (c) the delivery and deployment of μCLIP mPDC stents [138], (d) the mechanical properties of μCLIP mPDC stents [139], and (e) the biodegradation of DLP mPDC stents [140].

same group of researchers later developed a self-healing SMP for 4D printing [146]. They suggested that the potential applications of this polymer include cardiovascular stents that have developed damages. In this approach, damaged stents will self-repair once exposed to heat. Bodaghi *et al.* [147] used MJ to co-print two types of SMP with low and high glass transition temperatures to create sequential responses upon exposure to temperature variations. The printed stents deployed when heating in water to 90 °C. Wan *et al.* [148] used DIW to fabricate a 4D shape-changing stent from biocompatible poly(D,L-lactide-co-trimethylene carbonate) (PLMC). The stent showed a restrictive shape recovery process within 35 s at 40 °C (Fig. 11**c**). Lin *et al.* [149] used FDM-based 4D printing to create two types of personalized shape-memory vascular stents with a negative Poisson's ratio. The recovery ratio of the stents was as high as 98% and the response time was only 5 s at 70 °C (Fig. 11**d**). Zhou *et al.* [150] applied RMS-AM for the 4D printing of a drug-loaded vascular PCL stent (Fig. 11**e**). The stent showed good biocompatibility and mechanical properties that were comparable to commercial stents. Zhang *et al.* [151] demonstrated 4D printing of a new SMP, named poly(glycerol dodecanoate) acrylate (PGDA) with a transformation temperature in the range of 20 to 37°C, for potential application as geometrically adaptive vascular stents. The printed stents showed shape memory properties, including a large fixity ratio of 100% at 20°C, a large recovery ratio of 98% at 37°C, a stable cyclability of $>$ 100 times, and a fast recovery speed of 0.4 s at 37°C, making it suitable for vascular stents and grafts in the human body environment (Fig. 11**f**). In 2021, van Manen *et al.* [152] presented a single-step RMS-AM-based 4D printing process for the fabrication of reconfigurable PLA stents using a modified commercial FDM printer. Unlike all the preceding studies, they demonstrated the possibility of producing deployable bifurcation stents by 4D printing that would otherwise be extremely challenging to create. The shape-shifting behavior could be completed in 30 s at 90 °C (Fig. 12**a**). Kitana *et al.* [153] employed DIW for the 4D printing of a T-shaped vascular bifurcation stent from shape-changing hydrogel layers (Fig. 12**b**). The achieved stent diameters were comparable to those of native blood vessels. The inner surface of the stents showed good biocompatibility with HUVECs. In 2022, Zhao *et al.* [154] reported origami-derived self-assembly stents fabricated *via* FDM 4D printing from PLA. Origami greatly increased the stent shrinkage ratio from 40 to 94%. The recovery ratio of the printed stents was $>$ 85% and up to 97% at 60°C (Fig. 12**c**).

By far, most of the 4D printed vascular stents have been at the proof-of-concept stage. SMPs are the most commonly used materials for the fabrication of 4D-printed stents. However, the recovery temperature of normal SMP is still higher than the temperature of the human body. The glass transformation temperature of SMP must be further lowered in the future studies to make them viable clinically. Furthermore, more vascular-stent-related properties need to be evaluated *in vitro* and *in vivo*.

3.7. Post treatments

After fabrication, there are a series of post treatments that can be applied to modify the microstructure and improve the mechanical properties, surface characteristics, and biocompatibility of AM stents. For LB-PBF metallic stents, high-intensity laser may cause instability of the melt pool and a very high cooling rate, leading to increased porosity, significant residual stress, and high surface roughness. Heat treatment may be applied to modify the as-built microstructure and improve the mechanical properties of AM

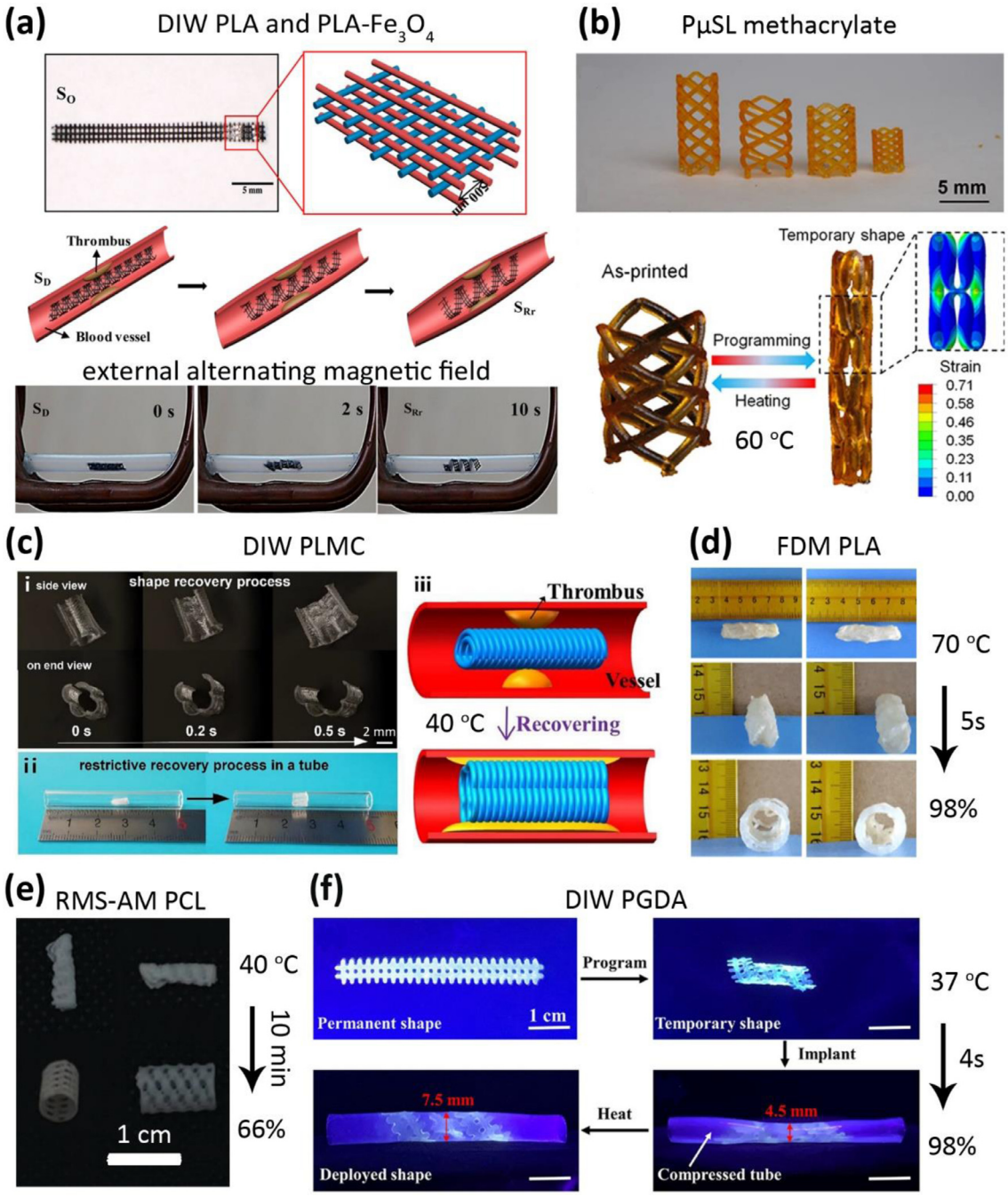

Fig. 11. 4D printed vascular stents: (a) DIW PLA and PLA/Fe_3O_4 composite stents recover to the original shape when exposed to the heating [144], (b) PμSL methacrylate-based copolymer stents recover to the original shape after heating [145], (c) the restrictive recovery process of DIW PLMC stents after heating [148], (d) FDM PLA stents recover to the original shape after heating [149], (e) RMS-AM PCL stents recover to the original shape after heating [150], and (f) the deployment of DIW PGDA stents after heating [151].

stents. For example, Finazzi et al. [155] found that the heat treatment helped dissolve the precipitates present in the matrix of LB-PBF NiTi micro-struts and provided the condition necessary for desired superelasticity. Langi et al. [92] suggested that the mechanical properties of LB-PBF 316L stents could be improved through a heat treatment process during which the columnar microstructure transformed into a fully equiaxed grain microstructure through recrystallization, accompanied by dislocation density reduction and residual stress relief. Moreover, since surface roughness plays an important role in the biocompatibility of AM stents, electrochemical polishing, sand blasting, or manual grinding followed by polishing is needed to achieve a smooth surface finish. Demir et al. [87] reduced the surface roughness (*Ra*) of LB-PBF CoCr stent to 1.45±0.09 μm by means of electrochemical polishing. Langi et al. [92] applied electrochemical polishing to LB-PBF NiTi stents and decreased *Ra* from 8.45 μm to 5.96 μm. Paul et al. [156] investigated the effects of microblasting on the properties of LB-PBF Fe-30Mn-1C-0.025S stent. They found that microblasting with glass beads and angular corundum particles reduced the stent *Ra* from 3.27 to 2.66 and 2.34, respectively, while higher concentrations of Si-, Na-, Ca-, and Al-oxides were detected on the stent surface that came from the blasting material. Meanwhile, both microblasted surfaces reduced SMC adhesion and change SMC morphology compared to the as-built state, which may be benefi-

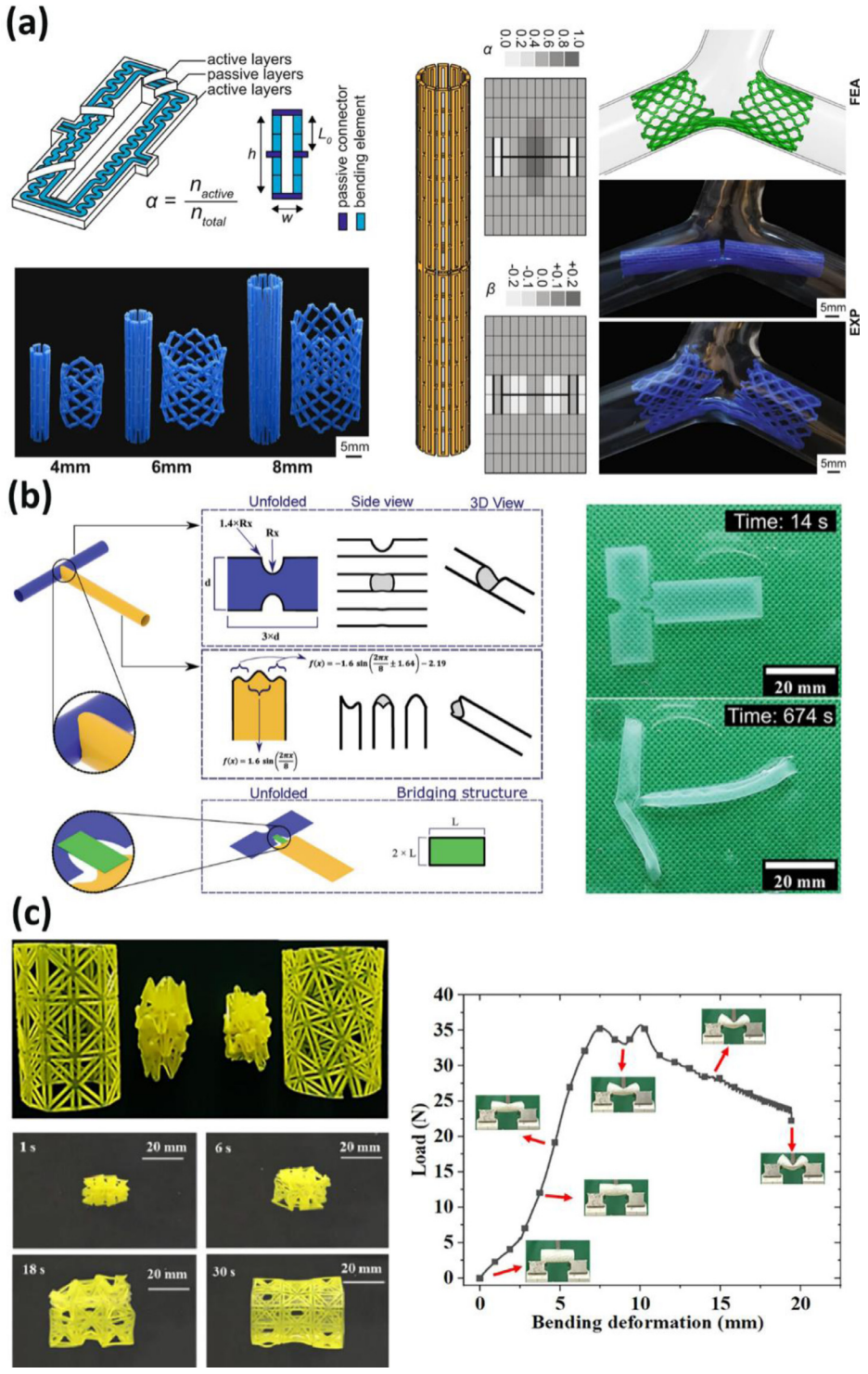

Fig. 12. Advanced 4D printed vascular stents: (a) RMS-AM deployable bifurcation PLA stents [152], (b) the formation of bifurcation stents in the water through shape-changing DIW hydrogel layers [153], and (c) FDM origami-derived self-assembly PLA stents and their bending performance [154].

cial regarding ISR. However, a further reduction of surface roughness is needed to achieve an expected *Ra* value of < 0.5 μm for biomedical applications. Also, the effects of surface treatment on the mechanical properties and degradation behavior of AM stents need to be further investigated. Similarly, for AM polymeric stents, post treatments are also necessary to achieve good mechanical properties and smooth surface. For instance, VP stents normally need a post curing process, such as extra UV irradiation [138] or heating [140], for better mechanical properties. Surface treatment, such as chemical etching, may be applied to reduce the surface roughness of the as-printed polymeric stents. Cabrera et al. [123] flattened the curved and nonuniform strut profile of FDM TPC stent with chloroform. They also found that the mechanical properties of the FDM TPC dog bone samples were not affected by the chemical etching with chloroform for 60s.

Table 2
The characteristics of the typical AM stents reported in the literature.

AM	Materialtype	Stent thickness(μm)	Support	Surface	Post treatment	Design
LB-PBF [89,95,103]	metals	>100	yes	rough	heat treatment, electropolishing	
SLS [108,111]	polymers	>180	no	rough	spraying or dip coating	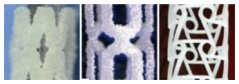
MJ [119,120]	polymers	>400	yes	smooth	support removal	
FDM [123,125]	polymers	>400	yes	rough	chloroform treating or support dissolving	
RMS-AM [127,130,131]	polymers	>60	no	smooth	-	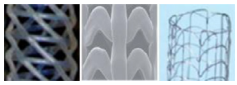
RMS-DIW [134]	polymers	>124	no	smooth	-	
μCLIP [138]	polymers	>150	yes	smooth	UV post curing	
DLP [140]	polymers	>500	yes	smooth	UV post curing	

4. Discussion

4.1. Stent design and manufacturing

An ideal stent should have high radial stiffness to minimize elastic recoil and good axial flexibility to achieve conformal shapes while being delivered through blood vessels and after deployment to reduce the complications during and after implantation. However, these two requirements are often incompatible, since increasing the radial stiffness normally decreases the axial flexibility of the stent. Therefore, a trade-off is needed to balance these properties. The design of the stent structure has a strong impact on the mechanical properties and should, therefore, be optimized to balance these properties and improve the performance of stents. Creative design ideas to reach the optimum balance between the mechanical properties along radial and axial directions can be realized using AM techniques. In addition, AM allows for fast iterations when trying to optimize the design of the stent structure. Moreover, it enables the customization of the stent geometry according to the specific curvature of the target blood vessel. The designs of vascular stent can typically be divided into two categories: 1. bridge type and 2. representative unit cell type. The desired mechanical properties of stents can be obtained by adjusting the design of the unit cell [157]. Recently, AM has been applied to develop stents with different structures based on the diamond, arrow, and auxetic unit cells (Table 2) [87,96,128,139]. However, most studies published to date seem to be of exploratory and proof-of-concept natures study without detailed biomechanical analysis beforehand. Moreover, most currently available studies do not exploit the full potential of AM techniques, as their focus seems to have primarily been on prototyping cylindrical stents with ordinary designs. There is, therefore, a substantial room to improve and optimize the current designs. It is suggested that future studies use topology optimization to improve the mechanical properties of stents. Moreover, creative design concepts, such as origami and kirigami, can be adopted to design AM stents [154]. 4D printed stents have appeared in the literature only very recently. Their design strategies need to be further developed so that the structure, shape, properties, and functionalities of stents can be effectively changed with time [152].

In addition to considerations regarding the performance of stents, one needs to consider the effects of various design concepts on the manufacturability of stents. While AM techniques can generally handle complex geometries, manufacturability is also dependent on the AM-processability of the required materials and as well as the geometrical fidelity and surface roughness of the end product. Densification and surface morphology of metallic lattice structure, for example, depend mainly on the energy density applied during LB-PBF [158–160]. The quality of overhanging structures can be improved by preheating the substrate, optimizing the scanning strategy, or adding surface-active elements, such as boron and niobium to reduce the surface tension of melt pool during LB-PBF [158]. There are currently no widely available AM techniques that can satisfy all the requirements for the fabrication of vascular stents. If a stent design involves large overhangs, a support structure is needed for most AM techniques (*e.g.*, LB-PBF, FDM, MJ, and SLA) (Table 2). When using these AM techniques, large overhangs should be avoided whenever possible, because removing the support structure will inevitably affect the surface roughness and even the structural integrity of the final product [161]. Design rules concerning inclinations and feature dimensions need to be followed to realize support-free stent fabrication [89]. Besides, RMS-AM can print stents without a support structure. However, it is limited in terms of the complexity of the printable unit cells. Therefore, in addition to BJ [112] and SLS, where the powder bed acts as a support, additional support-free AM techniques need to be developed. The availability of such support-free techniques would lead to an even higher degree of freedom in the geometrical design of stents.

The selection of AM techniques is dependent on the materials chosen for stents. In the literature, all AM metallic stents have been fabricated by using LB-PBF to take advantage of its high energy density and printing resolution. BJ may also be a choice for

metallic stents as long as the sintering process can be optimized to reduce the porosity and the shrinkage can be precisely controlled. For polymeric stents, a variety of AM techniques have been adopted, such as SLS, MJ, FDM, DIW, DLP, and SLA, depending on the polymerization mechanisms. SLS and FDM are suitable for thermoplastic polymers such as PLA and PLC, while MJ, DLP, and SLA require the resin to be photocurable.

Another important consideration in the design of stents is the printing resolution. The minimum dimensions of the stent struts are limited by the resolution of the applied AM technology. For instance, common LB-PBF machines can only print metal struts with a minimum thickness of 200 µm, while dedicated LB-PBF machines operating in the pulsed laser mode or with a small laser beam spot size can print struts with thicknesses below 100 µm [162,163]. Recently developed high-precision AM techniques, such as two-photon polymerization (2PP), allow for minimum feature sizes as small as 100 nm [164]. Other AM methods with higher printing resolutions need to be explored and developed for stent fabrication. Up till now, AM stents have been developed mostly for cardiovascular applications. Compared to cardiovascular vessels, intracranial arteries are much more tortuous with a diameter of only several millimeters in some cases [2]. Once such high-resolution printing methods have technologically matured, patient-specific stents with rationally designed unit cells will start to make inroads into the fight against cerebrovascular diseases as well.

4.2. Mechanical properties

The mechanical properties of stents play important roles in determining their effectiveness in the treatment of vascular lesions. In addition to the radial force and bending flexibility, typical bench tests for vascular stents include those required for evaluating their conformability, radial elastic recoil, and axial foreshortening. Radial force refers to the force generated by the stent which is applied to the artery to resist compression. This force should be high enough to integrate the thrombus into the blood vessel but not too high to avoid damaging the tissue. Bending flexibility represents the axial bending capacity of vascular stents. Stents need to have good bending flexibility not only because stents need to pass through torturous blood vessels but also because they need to adapt their shape to the curvature of the targeted section of blood vessels. Conformability is the ability of the stent to adapt its shape to that of the vascular wall. Stents typically need to match the shape of the targeted section of blood vessels both in terms of the cross-section profile and curvature. Proper function of stents, therefore, requires sufficient radial force and bending flexibility. Radial elastic recoil is an important property index for balloon-expandable stents. After expansion, stents retract radially once the balloon is deflated and withdrawn. The final diameter of a stent is, thus, determined by its elastic recoil. Generally, minimum elastic recoil is preferred. Axial foreshortening happens with the expansion of the stent as a consequence of which the axial length of the stent decreases. Low foreshortening is desired, because a much-shortened stent may lead to placement failure (Fig. 13**a**).

In addition to the stent material and design, the mechanical properties of AM stents strongly depend on the stent quality. The quality metrics of AM stents include strut density, fidelity, surface roughness, inter-layer bonding, and anisotropy. Optimization of the AM process, prior to the fabrication of vascular stents, is typically the first step to take in order to achieve high quality AM stents. For example, the process engineer must fine-tune the parameters of the LB-PBF process, including laser power, scanning speed, hatching distance, and layer thickness [89] to meet the quality requirements. The optimization of AM processes is currently largely based on the operator's experience, making it time-consuming and cost-ineffective. *In-situ* process monitoring and machine learning-based predictive models should, therefore, be incorporated into AM process optimization [165]. In addition, new AM techniques must be developed. µCLIP is a good example. As a variant of VP processes, it allows for continuous building of stents and can avoid inter-layer steps caused by layer-by-layer printing [166]. Moreover, post-AM treatments need to be developed for the applied AM processes to improve the mechanical properties and surface quality of the final products.

In the majority of the studies published to date, researchers have analyzed the radial force of AM stents. More comprehensive mechanical characterization of AM stents needs to be performed. In addition to static mechanical properties, vascular stents experience physiological pulsatile contact pressures in arteries, which may cause long-term high-cycle fatigue failure. Future studies should, therefore, also study the (corrosion) fatigue behavior of stent. AM BRS stents are particularly susceptible to the effects of both static and cyclic loading. That is because there may be significant mutual effects between biodegradation process on the one hand and the static and dynamic stresses developed in the stents on the other hand. Quasi-static and fatigue experiments should, therefore, be performed in physiologically relevant environments to characterize the biodegradation-dependent mechanical properties of such stents (Fig. 13**a**).

4.3. Biological properties

AM stents should have excellent multi-faceted biological properties to be hemocompatible, to promote endothelialization, and to avoid ISR and ST. Conventionally manufactured BMS are susceptible to thrombogenesis, restenosis, and hypersensitivity. BMS stay permanently in the blood vessel and may act as a site for platelet adhesion, leading to blood coagulation. Moreover, metallic ions released from stents (*e.g.*, Ni ions) may cause allergic responses and even genotoxic effects. Nickel-free metallic biomaterials are, therefore, suggested by some researchers [32] for producing BMS stents. DES can inhibit hyperplasia of SMCs through drug eluting, while the risk of late thrombosis is increased because of delayed healing and induced inflammation. BRS have been developed to further improve the biological properties of vascular stents. Bioresorbable polymers are generally considered to be hemocompatible, as their degradation products can be safely metabolized. On the other hand, some inflammatory responses, which may be attributed to the bulk-erosion behavior of polymers, have been reported [167]. The bioresorbable metals that have been studied for stent applications are among the essential elements of the human body and are reported to promote tissue regeneration and to limit SMC growth [168]. In addition, the biodegradation mode of metals tends to be layer-wise and starting from the surface, which is different from the bulk-erosion behavior observed in many biopolymers that could lead to unpredictable and sudden loss of their mechanical integrity. Biodegradable metals, therefore, hold great promise for application as stent material, as along as uniform, surface corrosion is their primary mode of biodegradation *in vivo*.

Since AM stents are at the very early stage of their development, most of the studies have not entered the stage of *in vitro* cytocompatibility or hemocompatiblity tests. While some *in vitro* studies, indeed, show that AM stents have good biocompatibility, *in vivo* conditions may differ greatly from the *in vitro* ones. In addition to the material, the manufacturing quality, surface roughness, and unit cell design can also affect the biological performance of AM stents. For instance, Habibzadeh et al. [169] found that electrochemical polishing improved the surface biocompatibility and hemocompatibility of 316L stainless steel, which could be attributed to the decreased surface roughness and increased corrosion resistance. Atapour et al. [170] compared the biocompatibility of the as-build and as-polished AM CoCrMo strut surfaces and

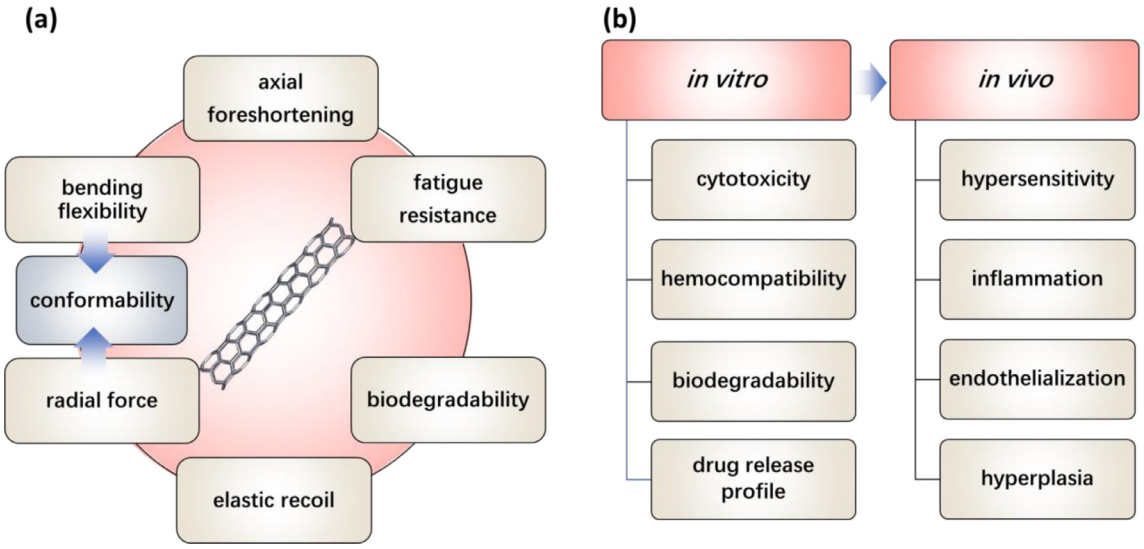

Fig. 13. The mechanical, functional, and biological properties of AM vascular stents.

found higher bioactivity (adsorption of hydroxyapatite) and slightly higher cell viability on the as-built surface, although there was no statistically significant difference between these two groups. Future development of AM stents should aim at achieving biomechanical and physicochemical properties that are comparable to commercial stents. They should also exhibit the required biological properties *in vivo* (Fig. 13**b**). Furthermore, studies on surface modification and drug-loading/release must be performed with the aim of improving the biological performance of AM metallic stents.

5. Conclusions

AM provides unprecedented opportunities for the development of personalized biomedical devices. The recent progress in the development of AM technologies has triggered many efforts to fabricate vascular stents through different AM approaches and from different materials. Almost all of the commercially used stent materials, such as bio-inert metals, bioresorbable polymers, and bioresorbable metals, have been applied to develop AM vascular stents. Among the applicable AM techniques, LB-PBF is appropriate for metallic stent fabrication, while SLA, FDM, DLP, and MJ can build polymeric stents. AM has demonstrated its potential advantage in generating customized stents with unique unit cell designs, which will lead to better conformability as well as improved crimping-expansion performance. Moreover, some of AM stents have shown good *in vitro* biocompatibility and mechanical properties that are comparable to their commercial counterparts. Although AM stents are still at the early stages of development, a clinical trial of FDM polymer stents has been already performed. Obviously, many technological barriers are still present and need to be removed before the clinical application of AM vascular stents.

6. Future directions

The future research directions to deal with the technological barriers that have inhibited the clinical adoption of AM vascular stents include the following:

(1) From the materials viewpoint, more AM-suitable biocompatible materials need to be developed to broaden the repertoire of available materials for AM stents. For example, stents made of biodegradable metals (*e.g.*, Zn, Mg, and Fe) can be developed using LB-PBF or BJ. Photocurable bioinks with high biocompatibility and mechanical properties can be developed by using VP. Moreover, functional drugs can be incorporated into the base materials of AM stents to enhance their biological performance.

(2) From the manufacturing viewpoint, current AM processes need to be further improved to realize desired strut thickness, strut density, surface roughness, and mechanical properties of AM stents. For instance, the printing quality can be further optimized based on the physical modelling and machine learning guided parameter optimization. High-resolution printing can be developed to fabricate vascular stents with thinner strut thickness and better surface roughness. More support-free AM techniques must be developed to minimize the limitations imposed on the rational design of stents and to achieve a smooth surface. Post-AM treatment is also very important for improving the surface smoothness and mechanical properties of AM stents. Combinational surface treatments with electrochemical, mechanical, and plasma polishing need to be developed to meet the required roughness.

(3) More advanced AM technologies need to be developed and applied to fabricate vascular stents with unique properties. Multi-material printing and 4D printing must be adopted to develop stents for some special conditions, *e.g.*, bifurcated, fragile, or atypical blood vessels.

(4) AM-enabled new designs will open new horizons for the development of vascular stents. Creative design concepts (*e.g.*, origami, kirigami, or auxetic designs) can be adopted for the design of stents to achieve better conformability and crimping-expansion behavior.

The success in the development of AM vascular stents also requires systematic studies regarding their biomechanical and biological performances. With continued rapid progress in the development of both AM materials and AM techniques, AM vascular stents are expected to revolutionize the treatment of vascular diseases in the coming years.

Declaration of Competing Interest

The authors declare that they have no known competing financial interests or personal relationships that could have appeared to influence the work reported in this paper.

Acknowledgements

The work was financially supported by the National Natural Science Foundation of China (52201294), China Postdoctoral Science Foundation (2022M710345), Natural Science Foundation of Beijing (L212014), and Fundamental Research Funds for the Central Universities and the Youth Teacher International Exchange & Growth Program (No. QNXM20220022).

References

[1] S.H. Im, D.H. Im, S.J. Park, Y. Jung, D.-H. Kim, S.H. Kim, Current status and future direction of metallic and polymeric materials for advanced vascular stents, Prog. Mater. Sci. 126 (2022) 100922.
[2] M. Li, M. Jiang, Y. Gao, Y. Zheng, Z. Liu, C. Zhou, T. Huang, X. Gu, A. Li, J. Fang, X. Ji, Current status and outlook of biodegradable metals in neuroscience and their potential applications as cerebral vascular stent materials, Bioact. Mater. 11 (2022) 140–153.
[3] E.S. Donkor, Stroke in the 21st century: a snapshot of the burden, epidemiology, and quality of life, Stroke Res. Treat. (2018) 3238165 2018.
[4] G.J. Ughi, M.G. Marosfoi, R.M. King, J. Caroff, L.M. Peterson, B.H. Duncan, E.T. Langan, A. Collins, A. Leporati, S. Rousselle, D.K. Lopes, M.J. Gounis, A.S. Puri, A neurovascular high-frequency optical coherence tomography system enables in situ cerebrovascular volumetric microscopy, Nat. Commun. 11 (1) (2020) 3851.
[5] A.D. Lopez, C.D. Mathers, M. Ezzati, D.T. Jamison, C.J.L. Murray, Global and regional burden of disease and risk factors, 2001: systematic analysis of population health data, Lancet North Am. Ed. 367 (9524) (2006) 1747–1757.
[6] S.C. Smith, A. Collins, R. Ferrari, D.R. Holmes, S. Logstrup, D.V. McGhie, J. Ralston, R.L. Sacco, H. Stam, K. Taubert, D.A. Wood, W.A. Zoghbi, Our time: a call to save preventable death from cardiovascular disease (heart disease and stroke), Circulation 126 (23) (2012) 2769–2775.
[7] WHO, Cardiovascular diseases (CVDs), 2021. https://www.who.int/news-room/fact-sheets/detail/cardiovascular-diseases-(cvds). (Accessed 11.11 2022).
[8] R. Khalaj, A.G. Tabriz, M.I. Okereke, D. Douroumis, 3D printing advances in the development of stents, Int. J. Pharm. 609 (2021) 121153.
[9] D.J. Kereiakes, Y. Onuma, P.W. Serruys, G.W. Stone, Bioresorbable vascular scaffolds for coronary revascularization, Circulation 134 (2) (2016) 168–182.
[10] R. Holzer, Z.M. Hijazi, Interventional approach to congenital heart disease, Curr. Opin. Cardiol. 19 (2) (2004) 84–90.
[11] C.-J. Chen, D. Ding, R.M. Starke, P. Mehndiratta, R.W. Crowley, K.C. Liu, A.M. Southerland, B.B. Worrall, Endovascular vs medical management of acute ischemic stroke, Neurology 85 (22) (2015) 1980–1990.
[12] L. Yang, X. Chen, L. Zhang, L. Li, S. Kang, C. Wang, W. Sun, Additive manufacturing in vascular stent fabrication, MATEC Web Conf. 253 (2019) 03003.
[13] W. Jiang, W. Zhao, T. Zhou, L. Wang, T. Qiu, A review on manufacturing and post-processing technology of vascular stents, Micromachines 13 (1) (2022) 140.
[14] C. Li, D. Pisignano, Y. Zhao, J. Xue, Advances in medical applications of additive manufacturing, Engineering 6 (11) (2020) 1222–1231.
[15] A.A. Zadpoor, Mechanical performance of additively manufactured meta-biomaterials, Acta Biomater. 85 (2019) 41–59.
[16] N. Muhammad, A.A. Azli, M.S. Saleh, M.N.A. Salimi, M.F. Ghazli, S.Z.A. Rahim, A review on additive manufacturing in bioresorbable stent manufacture, AIP Conf. Proc. 2347 (1) (2021) 020040.
[17] W. Hua, W. Shi, K. Mitchell, L. Raymond, R. Coulter, D. Zhao, Y. Jin, 3D printing of biodegradable polymer vascular stents: a review, Chin. J. Mech. Eng.: Addit. Manuf. Front. 1 (2) (2022) 100020.
[18] I. Cockerill, C.W. See, M.L. Young, Y. Wang, D. Zhu, Designing better cardiovascular stent materials: a learning curve, Adv. Funct. Mater. 31 (1) (2021) 2005361.
[19] R. Kornowski, M.K. Hong, F.O. Tio, O. Bramwell, H. Wu, M.B. Leon, In-stent restenosis: contributions of inflammatory responses and arterial injury to neointimal hyperplasia, J. Am. Coll. Cardiol. 31 (1) (1998) 224–230.
[20] P.K. Bowen, E.R. Shearier, S. Zhao, R.J. Guillory, F. Zhao, J. Goldman, J.W. Drelich, Biodegradable metals for cardiovascular stents: from clinical concerns to recent Zn-alloys, Adv. Healthc. Mater. 5 (10) (2016) 1121–1140.
[21] O.C. Marroquin, F. Selzer, S.R. Mulukutla, D.O. Williams, H.A. Vlachos, R.L. Wilensky, J.-F. Tanguay, E.M. Holper, J.D. Abbott, J.S. Lee, C. Smith, W.D. Anderson, S.F. Kelsey, K.E. Kip, A comparison of bare-metal and drug-eluting stents for off-label indications, N. Engl. J. Med. 358 (4) (2008) 342–352.
[22] R. Busch, A. Strohbach, S. Rethfeldt, S. Walz, M. Busch, S. Petersen, S. Felix, K. Sternberg, New stent surface materials: the impact of polymer-dependent interactions of human endothelial cells, smooth muscle cells, and platelets, Acta Biomater. 10 (2) (2014) 688–700.
[23] A. Tan, Y. Farhatnia, A. de Mel, J. Rajadas, M.S. Alavijeh, A.M. Seifalian, Inception to actualization: next generation coronary stent coatings incorporating nanotechnology, J. Biotechnol. 164 (1) (2013) 151–170.
[24] H. Hermawan, D. Dubé, D. Mantovani, Developments in metallic biodegradable stents, Acta Biomater. 6 (5) (2010) 1693–1697.
[25] M. Moravej, D. Mantovani, Biodegradable metals for cardiovascular stent application: interests and new opportunities, Int. J. Mol. Sci. 12 (7) (2011) 4250.
[26] Y.F. Zheng, X.N. Gu, F. Witte, Biodegradable metals, Mater. Sci. Eng. R Rep. 77 (2014) 1–34.
[27] K.H. Lo, C.H. Shek, J.K.L. Lai, Recent developments in stainless steels, Mater. Sci. Eng. R Rep. 65 (4) (2009) 39–104.
[28] Q. Chen, G.A. Thouas, Metallic implant biomaterials, Mater. Sci. Eng. R Rep. 87 (2015) 1–57.
[29] L. Gardner, Stability and design of stainless steel structures – review and outlook, Thin-Walled Struct. 141 (2019) 208–216.
[30] I. Cicha, C. Alexiou, Cardiovascular applications of magnetic particles, J. Magn. Magn. Mater. 518 (2021) 167428.
[31] J. Frattolin, E. Cattarinuzzi, S. Rajagopalan, D. Gastaldi, P. Vena, S. Yue, O.F. Bertrand, R. Mongrain, Development of a micro-scale method to assess the effect of corrosion on the mechanical properties of a biodegradable Fe-316L stent material, J. Mech. Behav. Biomed. Mater. 114 (2021) 104173.
[32] K. Yang, Y. Ren, Nickel-free austenitic stainless steels for medical applications, Sci. Technol. Adv. Mater. 11 (1) (2010) 014105.
[33] K. Kapnisis, G. Constantinides, H. Georgiou, D. Cristea, C. Gabor, D. Munteanu, B. Brott, P. Anderson, J. Lemons, A. Anayiotos, Multi-scale mechanical investigation of stainless steel and cobalt–chromium stents, J. Mech. Behav. Biomed. Mater. 40 (2014) 240–251.
[34] J.S. Saini, L. Dowling, D. Trimble, D. Singh, Mechanical properties of selective laser melted CoCr alloys: a review, J. Mater. Eng. Perform. 30 (12) (2021) 8700–8714.
[35] C. Delaunay, I. Petit, I.D. Learmonth, P. Oger, P.A. Vendittoli, Metal-on-metal bearings total hip arthroplasty: the cobalt and chromium ions release concern, Orthop. Traumatol. Surg. Res. 96 (8) (2010) 894–904.
[36] C. von Birgelen, P. Zocca, R.A. Buiten, G.A.J. Jessurun, C.E. Schotborgh, A. Roguin, P.W. Danse, E. Benit, A. Aminian, K.G. van Houwelingen, R.L. Anthonio, M.G. Stoel, S. Somi, M. Hartmann, G.C.M. Linssen, C.J.M. Doggen, M.M. Kok, Thin composite wire strut, durable polymer-coated (Resolute Onyx) versus ultrathin cobalt–chromium strut, bioresorbable polymer-coated (Orsiro) drug-eluting stents in allcomers with coronary artery disease (BIONYX): an international, single-blind, randomised non-inferiority trial, Lancet North Am. Ed. 392 (10154) (2018) 1235–1245.
[37] S. Bangalore, B. Toklu, N. Patel, F. Feit, G.W. Stone, Newer-generation ultrathin strut drug-eluting stents versus older second-generation thicker strut drug-eluting stents for coronary artery disease, Circulation 138 (20) (2018) 2216–2226.
[38] M.S. Patel, J.R. McCormick, A. Ghasem, S.R. Huntley, J.P. Gjolaj, Tantalum: the next biomaterial in spine surgery? J. Spine. Surg. 6 (1) (2020) 72–86.
[39] L. Zhou, T. Yuan, R. Li, J. Tang, G. Wang, K. Guo, Selective laser melting of pure tantalum: densification, microstructure and mechanical behaviors, Mater. Sci. Eng., A 707 (2017) 443–451.
[40] J. Black, Biologic performance of tantalum, Clin. Mater. 16 (3) (1994) 167–173.
[41] B.J. D, S.G. J, H.S. A, T. M, K.J. J, Characteristics of bone ingrowth and interface mechanics of a new porous tantalum biomaterial, J. Bone Joint Surg. Br. 81-B (5) (1999) 907–914.
[42] K.H. Barth, R. Virmani, E.P. Strecker, M.A. Savin, D. Lindisch, A.H. Matsumoto, G.P. Teitelbaum, Flexible tantalum stents implanted in aortas and iliac arteries: effects in normal canines, Radiology 175 (1) (1990) 91–96.
[43] O.F. Bertrand, R. Sipehia, R. Mongrain, J. Rodés, J.-C. Tardif, L. Bilodeau, G. Côté, M.G. Bourassa, Biocompatibility aspects of new stent technology, J. Am. Coll. Cardiol. 32 (3) (1998) 562–571.
[44] A. Wadood, Brief overview on nitinol as biomaterial, Adv. Mater. Sci. Eng. (2016) 4173138 2016.
[45] X. Wang, J. Yu, J. Liu, L. Chen, Q. Yang, H. Wei, J. Sun, Z. Wang, Z. Zhang, G. Zhao, J. Van Humbeeck, Effect of process parameters on the phase transformation behavior and tensile properties of NiTi shape memory alloys fabricated by selective laser melting, Addit. Manuf. 36 (2020) 101545.
[46] G.F. Andreasen, T.B. Hilleman, An evaluation of 55 cobalt substituted nitinol wire for use in orthodontics, J. Am. Dent. Assoc. 82 (6) (1971) 1373–1375.
[47] C.T. Dotter, R.W. Buschmann, M.K. McKinney, J. Rösch, Transluminal expandable nitinol coil stent grafting: preliminary report, Radiology 147 (1) (1983) 259–260.
[48] R.T. Higashida, V.V. Halbach, C.F. Dowd, L. Juravsky, S. Meagher, Initial clinical experience with a new self-expanding nitinol stent for the treatment of intracranial cerebral aneurysms: the cordis enterprise stent, Am. J. Neuroradiol. 26 (7) (2005) 1751–1756.
[49] C.-C. Shih, S.-J. Lin, Y.-L. Chen, Y.-Y. Su, S.-T. Lai, G.J. Wu, C.-F. Kwok, K.-H. Chung, The cytotoxicity of corrosion products of nitinol stent wire on cultured smooth muscle cells, J. Biomed. Mater. Res. 52 (2) (2000) 395–403.
[50] N. Sezer, Z. Evis, S.M. Kayhan, A. Tahmasebifar, M. Koç, Review of magnesium-based biomaterials and their applications, J. Magnes. Alloy. 6 (1) (2018) 23–43.
[51] D. Zhao, F. Witte, F. Lu, J. Wang, J. Li, L. Qin, Current status on clinical applications of magnesium-based orthopaedic implants: a review from clinical translational perspective, Biomaterials 112 (2017) 287–302.
[52] Y. Chen, Z. Xu, C. Smith, J. Sankar, Recent advances on the development of magnesium alloys for biodegradable implants, Acta Biomater. 10 (11) (2014) 4561–4573.
[53] M.-H. Kang, K.-H. Cheon, K.-I. Jo, J.-H. Ahn, H.-E. Kim, H.-D. Jung, T.-S. Jang, An asymmetric surface coating strategy for improved corrosion resistance and vascular compatibility of magnesium alloy stents, Mater. Des. 196 (2020) 109182.
[54] W.R. Zhou, Y.F. Zheng, M.A. Leeflang, J. Zhou, Mechanical property, biocorrosion and in vitro biocompatibility evaluations of Mg–Li–(Al)–(RE) al-

loys for future cardiovascular stent application, Acta Biomater. 9 (10) (2013) 8488–8498.
[55] L. Wang, G. Fang, L. Qian, S. Leeflang, J. Duszczyk, J. Zhou, Forming of magnesium alloy microtubes in the fabrication of biodegradable stents, Prog. Nat. Sci. 24 (5) (2014) 500–506.
[56] Y. Li, J. Wang, K. Sheng, F. Miao, Y. Wang, Y. Zhang, R. Hou, D. Mei, Y. Sun, Y. Zheng, S. Guan, Optimizing structural design on biodegradable magnesium alloy vascular stent for reducing strut thickness and raising radial strength, Mater. Des. 220 (2022) 110843.
[57] Q. Wang, G. Fang, Y.-H. Zhao, J. Zhou, Improvement of mechanical performance of bioresorbable magnesium alloy coronary artery stents through stent pattern redesign, Appl. Sci. 8 (12) (2018) 2461.
[58] M. Moravej, D. Mantovani, Biodegradable metals for cardiovascular stent application: interests and new opportunities, Int. J. Mol. Sci. 12 (7) (2011) 4250–4270.
[59] D. Bian, X. Zhou, J. Liu, W. Li, D. Shen, Y. Zheng, W. Gu, J. Jiang, M. Li, X. Chu, L. Ma, X. Wang, Y. Zhang, S. Leeflang, J. Zhou, Degradation behaviors and in-vivo biocompatibility of a rare earth- and aluminum-free magnesium-based stent, Acta Biomater. 124 (2021) 382–397.
[60] C. Rapetto, M. Leoncini, Magmaris: a new generation metallic sirolimus-eluting fully bioresorbable scaffold: present status and future perspectives, J. Thorac. Dis. 9 (Suppl 9) (2017) S903–s913.
[61] A. Francis, Y. Yang, S. Virtanen, A.R. Boccaccini, Iron and iron-based alloys for temporary cardiovascular applications, J. Mater. Sci. Mater. Med. 26 (3) (2015) 1–16.
[62] H. Hermawan, Updates on the research and development of absorbable metals for biomedical applications, Prog. Biomater. (2018).
[63] M. Peuster, C. Hesse, T. Schloo, C. Fink, P. Beerbaum, C. von Schnakenburg, Long-term biocompatibility of a corrodible peripheral iron stent in the porcine descending aorta, Biomaterials 27 (28) (2006) 4955–4962.
[64] R. Gorejová, L. Haverová, R. Oriňaková, A. Oriňak, M. Oriňak, Recent advancements in Fe-based biodegradable materials for bone repair, J. Mater. Sci. (2018).
[65] M. Peuster, P. Wohlsein, M. Brügmann, M. Ehlerding, K. Seidler, C. Fink, H. Brauer, A. Fischer, G. Hausdorf, A novel approach to temporary stenting: degradable cardiovascular stents produced from corrodible metal—results 6–18 months after implantation into New Zealand white rabbits, Heart 86 (5) (2001) 563–569.
[66] J.-F. Zheng, Z.-W. Xi, Y. Li, J.-N. Li, H. Qiu, X.-Y. Hu, T. Luo, C. Wu, X. Wang, L.-F. Song, L. Li, H.-P. Qi, G. Zhang, L. Qin, W.-Q. Zhang, X.-L. Shi, S.-H. Wang, D.-Y. Zhang, B. Xu, R.-L. Gao, Long-term safety and absorption assessment of a novel bioresorbable nitrided iron scaffold in porcine coronary artery, Bioact. Mater. 17 (2022) 496–505.
[67] W. Lin, H. Zhang, W. Zhang, H. Qi, G. Zhang, J. Qian, X. Li, L. Qin, H. Li, X. Wang, H. Qiu, X. Shi, W. Zheng, D. Zhang, R. Gao, J. Ding, In vivo degradation and endothelialization of an iron bioresorbable scaffold, Bioact. Mater. 6 (4) (2021) 1028–1039.
[68] H. Kabir, K. Munir, C. Wen, Y. Li, Recent research and progress of biodegradable zinc alloys and composites for biomedical applications: biomechanical and biocorrosion perspectives, Bioact. Mater. 6 (3) (2021) 836–879.
[69] G. Li, H. Yang, Y. Zheng, X.-H. Chen, J.-A. Yang, D. Zhu, L. Ruan, K. Takashima, Challenges in the use of zinc and its alloys as biodegradable metals: perspective from biomechanical compatibility, Acta Biomater. 97 (2019) 23–45.
[70] E. Mostaed, M. Sikora-Jasinska, J.W. Drelich, M. Vedani, Zinc-based alloys for degradable vascular stent applications, Acta Biomater. 71 (2018) 1–23.
[71] J. Venezuela, M.S. Dargusch, The influence of alloying and fabrication techniques on the mechanical properties, biodegradability and biocompatibility of zinc: a comprehensive review, Acta Biomater. 87 (2019) 1–40.
[72] P.K. Bowen, J. Drelich, J. Goldman, Zinc exhibits ideal physiological corrosion behavior for bioabsorbable stents, Adv. Mater. 25 (18) (2013) 2577–2582.
[73] Y.G.QIAN Yi, Research status, challenges, and countermeasures of biodegradable zinc-based vascular stents, Acta Metall. Sin. 57 (3) (2021) 272–282.
[74] C. Zhou, H.-F. Li, Y.-X. Yin, Z.-Z. Shi, T. Li, X.-Y. Feng, J.-W. Zhang, C.-X. Song, X.-S. Cui, K.-L. Xu, Y.-W. Zhao, W.-B. Hou, S.-T. Lu, G. Liu, M.-Q. Li, J.-y. Ma, E. Toft, A.A. Volinsky, M. Wan, X.-j. Yao, C.-b. Wang, K. Yao, S.-k. Xu, H. Lu, S.-F. Chang, J.-B. Ge, L.-N. Wang, H.-J. Zhang, Long-term in vivo study of biodegradable Zn-Cu stent: a 2-year implantation evaluation in porcine coronary artery, Acta Biomater. 97 (2019) 657–670.
[75] S. McMahon, N. Bertollo, E.D.O. Cearbhaill, J. Salber, L. Pierucci, P. Duffy, T. Dürig, V. Bi, W. Wang, Bio-resorbable polymer stents: a review of material progress and prospects, Prog. Polym. Sci. 83 (2018) 79–96.
[76] A.M. Sousa, A.M. Amaro, A.P. Piedade, 3D printing of polymeric bioresorbable stents: a strategy to improve both cellular compatibility and mechanical properties, Polymers 14 (6) (2022) 1099.
[77] Y. Bao, N. Paunović, J.-C. Leroux, Challenges and opportunities in 3D printing of biodegradable medical devices by emerging photopolymerization techniques, Adv. Funct. Mater. 32 (15) (2022) 2109864.
[78] W. Xu, M. Sasaki, T. Niidome, Sirolimus release from biodegradable polymers for coronary stent application: a review, Pharmaceutics 14 (3) (2022) 492.
[79] R.C. Eberhart, S.-H. Su, K.T. Nguyen, M. Zilberman, L. Tang, K.D. Nelson, P. Frenkel, Review: bioresorbable polymeric stents: current status and future promise, J. Biomater. Sci. Polym. Ed. 14 (4) (2003) 299–312.
[80] J. Lee, W.I. Choi, G. Tae, Y.H. Kim, S.S. Kang, S.E. Kim, S.-H. Kim, Y. Jung, S.H. Kim, Enhanced regeneration of the ligament–bone interface using a poly(l-lactide–co-ε-caprolactone) scaffold with local delivery of cells/BMP-2 using a heparin-based hydrogel, Acta Biomater. 7 (1) (2011) 244–257.
[81] D.Y. Kwon, J.I. Kim, D.Y. Kim, H.J. Kang, B. Lee, K.W. Lee, M.S. Kim, Biodegradable stent, J. Biomed. Sci. Eng. Vol.05 (No.04) (2012) 9.
[82] D. Battegazzore, S. Bocchini, A. Frache, Crystallization kinetics of poly(lactic acid)-talc composites, Express Polym. Lett. 5 (2011) 849–858.
[83] Á. Kmetty, T. Bárány, J. Karger-Kocsis, Self-reinforced polymeric materials: a review, Prog. Polym. Sci. 35 (10) (2010) 1288–1310.
[84] L.-Y. Chen, S.-X. Liang, Y. Liu, L.-C. Zhang, Additive manufacturing of metallic lattice structures: unconstrained design, accurate fabrication, fascinated performances, and challenges, Mater. Sci. Eng. R Rep. 146 (2021) 100648.
[85] D. Gu, X. Shi, R. Poprawe, D.L. Bourell, R. Setchi, J. Zhu, Material-structure-performance integrated laser-metal additive manufacturing, Science 372 (6545) (2021) eabg1487.
[86] S.A.M. Tofail, E.P. Koumoulos, A. Bandyopadhyay, S. Bose, L. O'Donoghue, C. Charitidis, Additive manufacturing: scientific and technological challenges, market uptake and opportunities, Mater. Today 21 (1) (2018) 22–37.
[87] A.G. Demir, B. Previtali, Additive manufacturing of cardiovascular CoCr stents by selective laser melting, Mater. Des. 119 (2017) 338–350.
[88] V. Finazzi, A.G. Demir, C.A. Biffi, C. Chiastra, F. Migliavacca, L. Petrini, B. Previtali, Design rules for producing cardiovascular stents by selective laser melting: geometrical constraints and opportunities, Procedia Struct. Integr. 15 (2019) 16–23.
[89] V. Finazzi, A.G. Demir, C.A. Biffi, F. Migliavacca, L. Petrini, B. Previtali, Design and functional testing of a novel balloon-expandable cardiovascular stent in CoCr alloy produced by selective laser melting, J. Manuf. Process 55 (2020) 161–173.
[90] M.A. Omar, B.T.H.T. Baharudin, S. Sulaiman, M.I.S. Ismail, M.A. Omar, Characterisation of powder and microstructure, density and surface roughness for additively manufactured stent using medical grade ASTM F75 cobalt chromium (CoCrMo) by selective laser melting (SLM) technology, Adv. Mater. Process. Technol. (2020) 1–12.
[91] E. Langi, A. Bisht, V.V. Silberschmidt, P.D. Ruiz, F. Vogt, L. Mailto, L. Masseling, L. Zhao, Characterisation of additively manufactured metallic stents, Procedia Struct. Integr 15 (2019) 41–45.
[92] E. Langi, L.G. Zhao, P. Jamshidi, M. Attallah, V.V. Silberschmidt, H. Willcock, F. Vogt, A comparative study of microstructures and nanomechanical properties of additively manufactured and commercial metallic stents, Mater. Today Commun. 31 (2022) 103372.
[93] K. Chen, H. Wan, X. Fang, H. Chen, Laser additive manufacturing of anti-tetrachiral endovascular stents with negative Poisson’s Ratio and favorable cytocompatibility, Micromachines 13 (7) (2022) 1135.
[94] L. Yan, S.L. Soh, N. Wang, Q. Ma, W.F. Lu, S.T. Dheen, A.S. Kumar, J.Y.H. Fuh, Evaluation and characterization of nitinol stents produced by selective laser melting with various process parameters, Prog. Addit. Manuf. (2022).
[95] V. Finazzi, F. Berti, R.J. Guillory Ii, L. Petrini, B. Previtali, A.G. Demir, Patient-specific cardiovascular superelastic NiTi stents produced by laser powder bed fusion, Procedia CIRP 110 (2022) 242–246.
[96] P. Jamshidi, C. Panwisawas, E. Langi, S.C. Cox, J. Feng, L. Zhao, M.M. Attallah, Development, characterisation, and modelling of processability of nitinol stents using laser powder bed fusion, J. Alloys Compd. 909 (2022) 164681.
[97] R. Wauthle, J. van der Stok, S. Amin Yavari, J. Van Humbeeck, J.-P. Kruth, A.A. Zadpoor, H. Weinans, M. Mulier, J. Schrooten, Additively manufactured porous tantalum implants, Acta Biomater. 14 (2015) 217–225.
[98] Y. Li, H. Jahr, K. Lietaert, P. Pavanram, A. Yilmaz, L.I. Fockaert, M.A. Leeflang, B. Pouran, Y. Gonzalez-Garcia, H. Weinans, J.M.C. Mol, J. Zhou, A.A. Zadpoor, Additively manufactured biodegradable porous iron, Acta Biomater. 77 (2018) 380–393.
[99] Y. Li, H. Jahr, P. Pavanram, F.S.L. Bobbert, U. Puggi, X.Y. Zhang, B. Pouran, M.A. Leeflang, H. Weinans, J. Zhou, A.A. Zadpoor, Additively manufactured functionally graded biodegradable porous iron, Acta Biomater. 96 (2019) 646–661.
[100] Y. Li, H. Jahr, J. Zhou, A.A. Zadpoor, Additively manufactured biodegradable porous metals, Acta Biomater. 115 (2020) 29–50.
[101] Y. Li, K. Lietaert, W. Li, X.Y. Zhang, M.A. Leeflang, J. Zhou, A.A. Zadpoor, Corrosion fatigue behavior of additively manufactured biodegradable porous iron, Corros. Sci. 156 (2019) 106–116.
[102] Y. Li, J. Shi, H. Jahr, J. Zhou, A.A. Zadpoor, L. Wang, Improving the mechanical properties of additively manufactured micro-architected biodegradable metals, JOM 73 (12) (2021) 4188–4198.
[103] B. Paul, A. Lode, A.-M. Placht, A. Voß, S. Pilz, U. Wolff, S. Oswald, A. Gebert, M. Gelinsky, J. Hufenbach, Cell–material interactions in direct contact culture of endothelial cells on biodegradable iron-based stents fabricated by laser powder bed fusion and impact of ion release, ACS Appl. Mater. Interfaces 14 (1) (2022) 439–451.
[104] Y. Li, H. Jahr, X.Y. Zhang, M.A. Leeflang, W. Li, B. Pouran, F.D. Tichelaar, H. Weinans, J. Zhou, A.A. Zadpoor, Biodegradation-affected fatigue behavior of additively manufactured porous magnesium, Addit. Manuf. 28 (2019) 299–311.
[105] Y. Li, P. Pavanram, J. Zhou, K. Lietaert, F.S.L. Bobbert, Y. Kubo, M.A. Leeflang, H. Jahr, A.A. Zadpoor, Additively manufactured functionally graded biodegradable porous zinc, Biomater. Sci. (2020).
[106] Y. Li, P. Pavanram, J. Zhou, K. Lietaert, P. Taheri, W. Li, H. San, M.A. Leeflang, J.M.C. Mol, H. Jahr, A.A. Zadpoor, Additively manufactured biodegradable porous zinc, Acta Biomater. 101 (2020) 609–623.
[107] Y. Li, J. Zhou, P. Pavanram, M.A. Leeflang, L.I. Fockaert, B. Pouran, N. Tümer, K.U. Schröder, J.M.C. Mol, H. Weinans, H. Jahr, A.A. Zadpoor, Additively

manufactured biodegradable porous magnesium, Acta Biomater. 67 (2018) 378–392.
[108] C. Flege, F. Vogt, S. Höges, L. Jauer, M. Borinski, V.A. Schulte, R. Hoffmann, R. Poprawe, W. Meiners, M. Jobmann, K. Wissenbach, R. Blindt, Development and characterization of a coronary polylactic acid stent prototype generated by selective laser melting, J. Mater. Sci. Mater. Med. 24 (1) (2013) 241–255.
[109] I. Gibson, D.W. Rosen, B. Stucker, M. Khorasani, D. Rosen, B. Stucker, M. Khorasani, Additive Manufacturing Technologies, Springer, 2021.
[110] W. Han, L. Kong, M. Xu, Advances in selective laser sintering of polymers, Int. J. Extreme Manuf. 4 (4) (2022) 042002.
[111] L.C. Geng, X.L. Ruan, W.W. Wu, R. Xia, D.N. Fang, Mechanical properties of selective laser sintering (SLS) additive manufactured chiral auxetic cylindrical stent, Exp. Mech. 59 (6) (2019) 913–925.
[112] A. Mostafaei, A.M. Elliott, J.E. Barnes, F. Li, W. Tan, C.L. Cramer, P. Nandwana, M. Chmielus, Binder jet 3D printing—process parameters, materials, properties, modeling, and challenges, Prog. Mater Sci. 119 (2021) 100707.
[113] D. Hong, D.-T. Chou, O.I. Velikokhatnyi, A. Roy, B. Lee, I. Swink, I. Issaev, H.A. Kuhn, P.N. Kumta, Binder-jetting 3D printing and alloy development of new biodegradable Fe-Mn-Ca/Mg alloys, Acta Biomater. 45 (2016) 375–386.
[114] K.X. Kuah, D.J. Blackwood, W.K. Ong, M. Salehi, H.L. Seet, M.L.S. Nai, S. Wijesinghe, Analysis of the corrosion performance of binder jet additive manufactured magnesium alloys for biomedical applications, J. Magnes. Alloy. 10 (5) (2022) 1296–1310.
[115] D. Ke, S. Bose, Effects of pore distribution and chemistry on physical, mechanical, and biological properties of tricalcium phosphate scaffolds by binder-jet 3D printing, Addit. Manuf. 22 (2018) 111–117.
[116] K. Sen, T. Mehta, S. Sansare, L. Sharifi, A.W.K. Ma, B. Chaudhuri, Pharmaceutical applications of powder-based binder jet 3D printing process – a review, Adv. Drug Del. Rev. 177 (2021) 113943.
[117] S. Vangapally, K. Agarwal, A. Sheldon, S. Cai, Effect of lattice design and process parameters on dimensional and mechanical properties of binder jet additively manufactured stainless steel 316 for bone scaffolds, Procedia Manuf. 10 (2017) 750–759.
[118] S. Mora, N.M. Pugno, D. Misseroni, 3D printed architected lattice structures by material jetting, Mater. Today (2022).
[119] S.S. Moore, K.J. O'Sullivan, F. Verdecchia, Shrinking the supply chain for implantable coronary stent devices, Ann. Biomed. Eng. 44 (2) (2016) 497–507.
[120] H. Xue, Z. Luo, T. Brown, S. Beier, Design of self-expanding auxetic stents using topology optimization, Front. Bioeng. Bio.Tech. 8 (2020).
[121] D. Popescu, A. Zapciu, C. Amza, F. Baciu, R. Marinescu, FDM process parameters influence over the mechanical properties of polymer specimens: a review, Polym. Test. 69 (2018) 157–166.
[122] V.C.-F. Li, C.K. Dunn, Z. Zhang, Y. Deng, H.J. Qi, Direct Ink Write (DIW) 3D printed cellulose nanocrystal aerogel structures, Sci. Rep. 7 (1) (2017) 8018.
[123] M.S. Cabrera, B. Sanders, O.J.G.M. Goor, A. Driessen-Mol, C.W.J. Oomens, F.P.T. Baaijens, Computationally designed 3D printed self-expandable polymer stents with biodegradation capacity for minimally invasive heart valve implantation: a proof-of-concept study, 3D print, Addit. Manuf. 4 (1) (2017) 19–29.
[124] H. Jia, S.-Y. Gu, K. Chang, 3D printed self-expandable vascular stents from biodegradable shape memory polymer, Adv. Polym. Tech. 37 (8) (2018) 3222–3228.
[125] Z. Wu, J. Zhao, W. Wu, P. Wang, B. Wang, G. Li, S. Zhang, Radial compressive property and the proof-of-concept study for realizing self-expansion of 3D printing polylactic acid vascular stents with negative Poisson's Ratio Structure, Materials 11 (8) (2018) 1357.
[126] Three-dimensional printing on a rotating cylindrical mandrel: a review of additive-lathe 3D printing technology, 3D print, Addit. Manuf. 6 (6) (2019) 293–307.
[127] S.A. Park, S.J. Lee, K.S. Lim, I.H. Bae, J.H. Lee, W.D. Kim, M.H. Jeong, J.-K. Park, In vivo evaluation and characterization of a bio-absorbable drug-coated stent fabricated using a 3D-printing system, Mater. Lett. 141 (2015) 355–358.
[128] A.J. Guerra, J. Ciurana, 3D-printed bioabsordable polycaprolactone stent: the effect of process parameters on its physical features, Mater. Des. 137 (2018) 430–437.
[129] A. Guerra, A. Roca, J. de Ciurana, A novel 3D additive manufacturing machine to biodegradable stents, Procedia Manuf. 13 (2017) 718–723.
[130] C. WANG, L. Zhang, Y. Fang, W. Sun, Design, characterization, and 3D printing of cardiovascular stents with zero Poisson's ratio in longitudinal deformation, Engineering 7 (7) (2021) 979–990.
[131] K. Somszor, O. Bas, F. Karimi, T. Shabab, N.T. Saidy, A.J. O'Connor, A.V. Ellis, D. Hutmacher, D.E. Heath, Personalized, mechanically strong, and biodegradable coronary artery stents via melt electrowriting, ACS Macro Lett. 9 (12) (2020) 1732–1739.
[132] Y. Shen, C. Tang, B. Sun, Y. Zhang, X. Sun, M. El-Newehy, H. El-Hamshary, Y. Morsi, H. Gu, W. Wang, X. Mo, 3D printed personalized, heparinized and biodegradable coronary artery stents for rabbit abdominal aorta implantation, Chem. Eng. J. 450 (2022) 138202.
[133] T. Yin, R. Du, Y. Wang, J. Huang, S. Ge, Y. Huang, Y. Tan, Q. Liu, Z. Chen, H. Feng, J. Du, Y. Wang, G. Wang, Two-stage degradation and novel functional endothelium characteristics of a 3-D printed bioresorbable scaffold, Bioact. Mater. 10 (2022) 378–396.
[134] V. Chausse, R. Schieber, Y. Raymond, B. Ségry, R. Sabaté, K. Kolandaivelu, M.-P. Ginebra, M. Pegueroles, Solvent-cast direct-writing as a fabrication strategy for radiopaque stents, Addit. Manuf. 48 (2021) 102392.
[135] Q. Ge, Z. Li, Z. Wang, K. Kowsari, W. Zhang, X. He, J. Zhou, N.X. Fang, Projection micro stereolithography based 3D printing and its applications, Int. J. Extreme Manuf. 2 (2) (2020) 022004.
[136] H.O.T. Ware, A.C. Farsheed, E. Baker, G. Ameer, C. Sun, Fabrication speed optimization for high-resolution 3D-printing of bioresorbable vascular scaffolds, Procedia CIRP 65 (2017) 131–138.
[137] J.R. Tumbleston, D. Shirvanyants, N. Ermoshkin, R. Janusziewicz, A.R. Johnson, D. Kelly, K. Chen, R. Pinschmidt, J.P. Rolland, A. Ermoshkin, E.T. Samulski, J.M. DeSimone, Continuous liquid interface production of 3D objects, Science 347 (6228) (2015) 1349–1352.
[138] R. van Lith, E. Baker, H. Ware, J. Yang, A.C. Farsheed, C. Sun, G. Ameer, 3D-printing strong high-resolution antioxidant bioresorbable vascular stents, Adv. Mater. Technol. 1 (9) (2016) 1600138.
[139] H.O.T. Ware, A.C. Farsheed, B. Akar, C. Duan, X. Chen, G. Ameer, C. Sun, High--speed on-demand 3D printed bioresorbable vascular scaffolds, Mater. Today Chem. 7 (2018) 25–34.
[140] M.F. de Oliveira, L.C.E. da Silva, M.G. de Oliveira, 3D printed bioresorbable nitric oxide-releasing vascular stents, Bioprinting 22 (2021) e00137.
[141] F. Momeni, S. M.Mehdi Hassani.N, X. Liu, J. Ni, A review of 4D printing, Mater. Des. 122 (2017) 42–79.
[142] X. Kuang, D.J. Roach, J. Wu, C.M. Hamel, Z. Ding, T. Wang, M.L. Dunn, H.J. Qi, Advances in 4D printing: materials and applications, Adv. Funct. Mater. 29 (2) (2019) 1805290.
[143] X. Wang, Y. Zhang, P. Shen, Z. Cheng, C. Chu, F. Xue, J. Bai, Preparation of 4D printed peripheral vascular stent and its degradation behavior under fluid shear stress after deployment, Biomater. Sci. 10 (9) (2022) 2302–2314.
[144] H. Wei, Q. Zhang, Y. Yao, L. Liu, Y. Liu, J. Leng, Direct-write fabrication of 4D active shape-changing structures based on a shape memory polymer and its nanocomposite, ACS Appl. Mater. Interfaces 9 (1) (2017) 876–883.
[145] Q. Ge, A.H. Sakhaei, H. Lee, C.K. Dunn, N.X. Fang, M.L. Dunn, Multimaterial 4D printing with tailorable shape memory polymers, Sci. Rep. 6 (1) (2016) 31110.
[146] B. Zhang, W. Zhang, Z. Zhang, Y.-F. Zhang, H. Hingorani, Z. Liu, J. Liu, Q. Ge, Self-healing four-dimensional printing with an ultraviolet curable double-network shape memory polymer system, ACS Appl. Mater. Interfaces 11 (10) (2019) 10328–10336.
[147] M. Bodaghi, A.R. Damanpack, W.H. Liao, Self-expanding/shrinking structures by 4D printing, Smart Mater. Struct. 25 (10) (2016) 105034.
[148] X. Wan, H. Wei, F. Zhang, Y. Liu, J. Leng, 3D printing of shape memory poly(d,l-lactide-co-trimethylene carbonate) by direct ink writing for shape-changing structures, J. Appl. Polym. Sci. 136 (44) (2019) 48177.
[149] C. Lin, L. Zhang, Y. Liu, L. Liu, J. Leng, 4D printing of personalized shape memory polymer vascular stents with negative Poisson's ratio structure: a preliminary study, Sci. China Technol. Sci. 63 (4) (2020) 578–588.
[150] Y. Zhou, Dong Zhou, P. Cao, X. Zhang, Q. Wang, T. Wang, Z. Li, W. He, J. Ju, Y. Zhang, 4D printing of shape memory vascular stent based on βCD-g-polycaprolactone, Macromol. Rapid Commun. 42 (14) (2021) 2100176.
[151] C. Zhang, D. Cai, P. Liao, J.-W. Su, H. Deng, B. Vardhanabhuti, B.D. Ulery, S.-Y. Chen, J. Lin, 4D printing of shape-memory polymeric scaffolds for adaptive biomedical implantation, Acta Biomater. 122 (2021) 101–110.
[152] T. van Manen, S. Janbaz, K.M.B. Jansen, A.A. Zadpoor, 4D printing of reconfigurable metamaterials and devices, Commun. Mater. 2 (1) (2021) 56.
[153] W. Kitana, I. Apsite, J. Hazur, A.R. Boccaccini, L. Ionov, 4D biofabrication of T-shaped vascular bifurcation, Adv. Mater. Technol. 8 (1) (2023) 2200429.
[154] W. Zhao, N. Li, L. Liu, J. Leng, Y. Liu, Origami derived self-assembly stents fabricated via 4D printing, Compos. Struct. 293 (2022) 115669.
[155] V. Finazzi, F. Berti, L. Petrini, B. Previtali, A.G. Demir, Additive manufacturing and post-processing of superelastic NiTi micro struts as building blocks for cardiovascular stents, Addit. Manuf. 70 (2023) 103561.
[156] B. Paul, A. Hofmann, S. Weinert, F. Frank, U. Wolff, M. Krautz, J. Edelmann, M.W. Gee, C. Reeps, J. Hufenbach, Effect of blasting treatments on the surface topography and cell adhesion on biodegradable FeMn-based stents processed by laser powder bed fusion, Adv. Eng. Mater. 24 (10) (2022) 2200961.
[157] C. Pan, Y. Han, J. Lu, Structural design of vascular stents: a review, Micromachines 12 (7) (2021) 770.
[158] H. Chen, D. Gu, J. Xiong, M. Xia, Improving additive manufacturing processability of hard-to-process overhanging structure by selective laser melting, J. Mater. Process. Technol. 250 (2017) 99–108.
[159] H. Chen, D. Gu, D. Dai, C. Ma, M. Xia, Microstructure and composition homogeneity, tensile property, and underlying thermal physical mechanism of selective laser melting tool steel parts, Mater. Sci. Eng., A 682 (2017) 279–289.
[160] H.-y. Chen, D.-d. Gu, Q. Ge, X.-y. Shi, H.-m. Zhang, R. Wang, H. Zhang, K. Kosiba, Role of laser scan strategies in defect control, microstructural evolution and mechanical properties of steel matrix composites prepared by laser additive manufacturing, Int. J. Min., Metall. Mater. 28 (3) (2021) 462–474.
[161] Y. Wang, J. Xia, Z. Luo, H. Yan, J. Sun, E. Lü, Self-supporting topology optimization method for selective laser melting, Addit. Manuf. 36 (2020) 101506.
[162] F. Guaglione, L. Caprio, B. Previtali, A.G. Demir, Single point exposure LPBF for the production of biodegradable Zn-alloy lattice structures, Addit. Manuf. (2021) 102426.
[163] Z. Xiong, H. Li, H. Yang, Y. Yang, Y. Liu, L. Cui, X. Li, L. Masseling, L. Shen, S. Hao, Micro laser powder bed fusion of NiTi alloys with superior mechanical property and shape recovery function, Addit. Manuf. 57 (2022) 102960.

[164] Q. Geng, D. Wang, P. Chen, S.-C. Chen, Ultrafast multi-focus 3-D nano-fabrication based on two-photon polymerization, Nat. Commun. 10 (1) (2019) 2179.
[165] C. Wang, X.P. Tan, S.B. Tor, C.S. Lim, Machine learning in additive manufacturing: state-of-the-art and perspectives, Addit. Manuf. 36 (2020) 101538.
[166] W. Li, L.S. Mille, J.A. Robledo, T. Uribe, V. Huerta, Y.S. Zhang, Recent advances in formulating and processing biomaterial inks for vat polymerization-based 3D printing, Adv. Healthc. Mater. 9 (15) (2020) 2000156.
[167] W.J.v.d. Giessen, A.M. Lincoff, R.S. Schwartz, H.M.M.v. Beusekom, P.W. Serruys, D.R. Holmes, S.G. Ellis, E.J. Topol, Marked inflammatory sequelae to implantation of biodegradable and nonbiodegradable polymers in porcine coronary arteries, Circulation 94 (7) (1996) 1690–1697.
[168] S.H. Im, Y. Jung, S.H. Kim, Current status and future direction of biodegradable metallic and polymeric vascular scaffolds for next-generation stents, Acta Biomater. 60 (2017) 3–22.
[169] S. Habibzadeh, L. Li, D. Shum-Tim, E.C. Davis, S. Omanovic, Electrochemical polishing as a 316L stainless steel surface treatment method: towards the improvement of biocompatibility, Corros. Sci. 87 (2014) 89–100.
[170] M. Atapour, S. Sanaei, Z. Wei, M. Sheikholeslam, J.D. Henderson, U. Eduok, Y.K. Hosein, D.W. Holdsworth, Y.S. Hedberg, H.R. Ghorbani, In vitro corrosion and biocompatibility behavior of CoCrMo alloy manufactured by laser powder bed fusion parallel and perpendicular to the build direction, Electrochim. Acta 445 (2023) 142059.